

Control of Surface Property for the Polymer/Agricultural Waste Composite Using Vapor-Phase Assisted Surface Polymerization (VASP)

著者	Lee Heesung
year	2014
その他のタイトル	気相重合法による農業残渣と高分子複合材料の界面制御
学位授与年度	平成25年度
学位授与番号	17104甲生工第214号
URL	http://hdl.handle.net/10228/5296

CONTROL OF SURFACE PROPERTY FOR THE
POLYMER/AGRICULTURAL WASTE COMPOSITE
USING VAPOR-PHASE ASSISTED SURFACE
POLYMERIZATION (VASP)

(気相重合法による農業残渣と高分子複合材料の界面制御)

LEE HEESUNG
10897002

PhD THESIS
2014

GRADUATE SCHOOL OF LIFE SCIENCE
AND SYSTEMS ENGINEERING
KYUSHU INSTITUTE OF TECHNOLOGY

Preface

This thesis deals with the studies accomplished by the author under the guidance by Associate Professor Minato Wakisaka, Associate Professor Tamaki Kato and Dr. Donghee Kim, Graduate School of Life Science and Systems Engineering, and Professor Haruo Nishida and Associate Professor Yoshito Andou, Eco-Town Collaborative R&D Center for the Environment and Recycling, Kyushu Institute of Technology, and Dr. Norio Nagasawa, NARO Bio-oriented Technology Research Advancement Institution.

LEE HeeSung
10897002

Graduate School of Life Science and
Systems Engineering,
Kyushu Institute of Technology
2-4 Hibikino, Wakamatsu, Kitakyushu
808-0196
Jap

ABSTRACT

In order to provide a valuable greener product using agricultural waste, polymer/ agricultural waste composites has been fabricated. Since, however, the incompatibility between the hydrophilic natural fiber and hydrophobic polymer matrices makes it difficult to disperse the individual fiber throughout polymer matrices, and the incorporation of agricultural waste into polymer matrices may compromise certain mechanical properties. In order to improve the compatibility between natural fiber and polymer matrices, this thesis is studied and discussed the control of surface property using compatibilizer and vapor phase assisted surface polymerization for the high-performance polymer/ agricultural waste composites. This thesis is composed of up to Chapter 5 from Chapter 1.

The background, scope and objectives of this study are described in the introduction Chapter 1.

In Chapter 2, in order to investigate potential of agricultural natural fiber as filler, I focused on *Erianthus arudinaceus* as a cellulose resource crop because of high CO₂ fixation efficiency. Polymer composites of polypropylene (PP) with *Erianthus* fiber (ETF) were fabricated and they were evaluated by mechanical properties to reveal the compatibility between PP and ETF. To overcome poor compatibility between PP and ETF, Maleic anhydride-modified polypropylene (MAPP) was applied as a compatibilizer. Since ETF/PP/MAPP composites improved the mechanical properties, it is revealed that interfacial property control between matrices and natural fibers is critical.

In Chapter 3, vapor-phase assisted surface polymerization (VASP) method was applied as an alternative approach to compatibilizer. The VASP is not only a surface coating method for fabrication of composites but it is also expected to be able to apply to a wide range of

substrates. VASP is an excellent method for preserving the fine structures of delicate substrate surfaces such as biomaterials in comparison with liquid and melting processes. After the diffusion and adsorption on the substrate surfaces, the monomer can be polymerized. . VASP of MMA onto wheat straw fiber (WSF) was applied to modify the surface property and improve the compatibility between PLLA and WSF. Bio-composites with biodegradable polymer (poly (L-lactic acid) (PLLA)) and WSF was fabricated via VASP. Since the PLLA/VWSF (treated with VASP in WSF) composites improved in tensile strength (20–30%) compared with that of PLLA/WSF composites, VASP proved to improve the compatibility between matrices and natural fibers.

In Chapter 4, the gas-flow type of vapor-phase assisted surface polymerization (VASP-F) was successfully developed since the substrate surface could be polymerized through monomer mist produced by monomer bubbling. VASP-F can inherit advantages of VASP method due to polymer grafted on substrate, and can recover non-reactant monomer. Larger amounts of substrate can be modified by VASP-F compared to VASP.

In conclusion, the improvement of compatibility between natural fiber and polymer matrices are essential to produce the high-performance polymer/agricultural waste composites.

This study provides new approach for the natural fiber reinforced plastics. The utilization of agricultural waste as filler for biocomposites would lead to the sustainable society throughout the achievement of environment conservation, and the social system encourage the agricultural sector revitalization.

TABLE OF CONTENTS

ABSTRACT	i
TABLE OF CONTENTS	iii
LIST OF TABLES	v
LIST OF FIGURES	vi
ABBREVIATION KEY	vii
CHAPTER 1. General introduction	1
1.1 Introduction	1
1.2 Fiber reinforced plastic (FRP)	1
1.3 Natural fiber reinforced polymer composites	3
1.4 Chemical surface modification	5
1.5 Vapor-phase assisted surface polymerization (VASP) method	6
1.6 Agricultural wastes	9
1.7 Research targets	9
1.8 References	11
CHAPTER 2. Development of biocomposites containing <i>Erianthus Arundinaceus</i> as cellulose resource crops	17
2.1 Introduction	17
2.2 Experimental	19
2.3 Results and discussion	23
2.4 Conclusion	33
2.5 Reference	34
CHAPTER 3. Enhancement of compatibility based on vapor-phase assisted surface polymerization (VASP) method for poly (L,L-lactide) composites with wheat straw fiber	37
3.1 Introduction	37
3.2 Experimental	39
3.3 Results and discussion	42
3.4 Conclusion	55
3.5 Reference	56
CHAPTER 4. Design of surface coating on powdery fiber by gas-flow type of vapor-phase assisted surface polymerization (VASP-F)	59
4.1 Introduction	59

4.2 Experimental	60
4.3 Results and discussion	64
4.4 Conclusion	73
4.5 Reference	74
CHAPTER 5. Conclusion	77
List of publication	79
Acknowledgement	81

LIST OF TABLES

Table 2-1. Volume distribution of <i>Erianthus</i> fibers (ETF) after sieving	20
Table 2-2. Characteristics of PP/ETF composites	26
Table 2-3. Characteristics of PP/ETF/MAPP composites	30
Table 3-1. VASP of methyl methacrylate (MMA) with AIBN on wheat straw fibers (WSF)	43
Table 3-2. Composition and SEC results of the PLLA composites containing WSF and VWSF	47
Table 4-1. Results of VASP-F of MMA on surface of wheat straw fibers (WSF)	64
Table 4-2. Results of VASP-F of MMA with varied reaction time	66
Table 4-3. Results of VASP-F of MMA on WSF in scale-up reactor	71

LIST OF FIGURES

Figure 1-1. Classification of lignocellulosic natural fibers	3
Figure 2-1. Photo Images of <i>Erianthus</i> (a), <i>Erianthus</i> stem (b), and the grinded <i>Erianthus</i> fibers (c)	20
Figure 2-2. TG curves of differential size of <i>Erianthus</i> fibers (ETF)	21
Figure 2-3. Chemical component of <i>Erianthus</i> fibers (ETF)	24
Figure 2-4. TG and DTG curves of <i>Erianthus</i> , rind, and inner stem	24
Figure 2-5. Effect of size distribution of fiber on the ETF/PP composites tensile strength and modulus (a), flexural strength and modulus (b)	27
Figure 2-6. Cross-section (Vertical direction is injection direction) images of PP/ETF and PP/ETF/MAPP composites using SEM: Entry 2(a), Entry 3(b), Entry 4(c), Entry 5(d), Entry 4-5(e), and Entry 5-3(f)	28
Figure 2-7. Influence of MAPP to ETF/PP composites tensile strength and modulus (a), flexural strength and modulus (b)	31
Figure 2-8. TG curves of PP, ETF, ETF/PP composites, and ETF/PP/MAPP	33
Figure 3-1. FT-IR spectra of PMMA (a), wheat straw fibers before (b) and after VASP of MMA (c), and extracted wheat straw fibers after VASP (d)	44
Figure 3-2. SEM images of wheat straw fibers before (a, b) and after VASP of MMA (c, d), and extracted wheat straw fibers after VASP (e, f)	45
Figure 3-3. TG and DTG thermographs of commercial PMMA and wheat straw fibers before and after VASP of MMA, and washed wheat straw fibers after VASP	46
Figure 3-4. TG (a) and DTG (b) thermographs of neat PLLA and wheat straw fibers before and after VASP of MMA filled PLLA composites	49
Figure 3-5. SEC profiles of PLLA/5, 15, 30 wt% WSF composites (a) and PLLA/5, 15, 30 wt% VWSF composites (b)	50
Figure 3-6. Tensile (a) and Flexural (b) data for PLLA with various amounts of WSF fibers	52
Figure 3-7. SEM images of PLLA / 15, 30 wt% WSF composites (a and b) and PLLA / 15, 30 wt% VWSF composites (c and d)	54
Figure 4-1. Schematic illustration of the VASP-F reaction system	61
Figure 4-2. FT-IR spectra of PMMA (a), wheat straw fibers before (b) and after VASP-F of MMA (Entry 1-5).	65
Figure 4-3. Relationship between the molecular weight and yield per initiator	67
Figure 4-4. Results of surface property of WSF before and after (Entry 1-4) VASP-F of MMA to water droplets	67
Figure 4-5. TG and DTG thermographs of commercial PMMA and WSF before and after VASP-F of MMA	69
Figure 4-6. FT-IR spectra of PMMA (a), wheat straw fibers before (b) and after VASP-F of MMA(c), and WSF after extraction with CHCl_3 (d)	70
Figure 4-7. FT-IR spectra of WSF (a), wheat straw fibers before (b) and after VASP-F of MMA(Entry 6-9)	72
Figure 4-8. SEM micrographs of wheat straw fibers before (a-b) and after VASP-F of MMA, Entry 8 (c, d)	73

ABBREVIATION KEY

ADMVN	2,2'-azobis(2, 4-dimethyl)valeronitrile
AIBN	2,2'-azobis(isobutyronitrile)
ETF	<i>Erianthus (Erianthus Arundinaceus)</i> fibers
Fig.	Figure
g	Gram
GPa	Giagapascal
MAPP	Maleic anhydride-modified polypropylene (MA-g-PP)
mg	Milligram
mg/g	Milligram per gram
mL	Milliliter
mL/h	Milliliter per hour
mL/min	Milliliter per minute
mm	Millimeter
mM	Millimol
MMA	Methyl methacrylate
M_n	Number-average molecular weight
M_w	Weight-average molecular weight
MPa	Megapascal
PLA	Polylactic acid
PLLA	Poly (<i>L,L</i> -lactide)
RH	Relative humidity
rpm	Rotations per minute
VASP	Vapor-phase assisted surface polymerization
VASP-F	Gas-flow type of vapor-phase assisted surface polymerization
WSF	Wheat straw fibers
wt %	Weight percent
μm	Micrometer
$^{\circ}\text{C}$	Temperature
%	Percentage

Chapter 1. General introduction

1.1 Introduction

Since global warming, ecological issues, depletion of fossil fuels, and air pollution have recently attracted a great deal of interest as serious environmental issues, the use of renewable biomass materials can significantly contribute a sustainable development [1-3]. The biomass materials are expected to contribute a key role for the reduction in carbon dioxide which induce reducing or decreasing energy consumption and dependency on fossil energy. It is attracting attention as one of the measures for depletion of petroleum resources and prevention of global warming. Many researchers in composite science have become increasingly interested in the usefulness of natural fibers as fillers and/or re-enforcers in plastic composites. Since their flexibility, highly specific stiffness, and low cost make them attractive as industrial materials, natural fiber reinforced plastic composites are attracting interest for their structural applications. Agricultural wastes are annually renewable wastes that can be valuable resources [4].

1.2 Fiber reinforced plastic (FRP)

The development of polymer composites has been driven by the need for the performance improvement with a specific combination of properties beyond those obtainable from a single material. These aims can be achieved in polymers through the use of copolymer

or blends, but the specific aspect that characterizes composite materials is that they are made up of distinct phases with very different physical properties. Although polymers are being employed more and more as structural materials, their use often is limited by their relatively low levels of stiffness and strength compared, for example, with metals.

Fiber reinforced plastics (FRP) is a composite material made of a polymer matrix reinforced with fibers. The most widely studied synthetic composite are focused upon polymers reinforced with stiff fibers and their use currently is increasing at the rate of 5%-10% per year across a range of different applications. Because of the need for light, stiff and strong materials for applications as diverse as aerospace structures and sporting goods, polymer-based high-performance composites have been developed over recent years with extremely impressive mechanical properties. The most impressive levels of reinforcement in polymer composites are obtained through the use of high-modulus fiber such as glass fiber and carbon fiber. A characteristic feature of fiber-reinforced composites is that, because of the complex arrangement of fibers, their mechanical properties are anisotropic. The reinforcement is controlled by both the geometry of fiber packing and the mechanical properties of the matrix polymer.

On the other hand, it is well known that the FRP is one of the most difficult materials to fractionate into elemental components, namely fiber, filler, and polymers in the waste recycling process. Therefore, the wastes are treated in the incineration or landfilling without any recycling approaches.

1.3 Natural fiber reinforced polymer composites

Amid growing environmental awareness around the world, the many researchers in industry and academic fields has focused on the use of greener products as environmentally benign materials. Therefore, many researchers have focused to use natural fibers as fillers and/or reinforcers in plastics composites. Since agricultural wastes are annual renewability, agricultural wastes can be valuable resources [5]. Their flexibility during processing, highly specific stiffness, and low cost (on a volumetric basis) make them attractive to manufacturers. In the recent decades, natural fibers as an alternative reinforcement in polymer composites have attracted the attention of many researchers and scientists due to their advantages over conventional glass and carbon fibers. The various advantages of natural fibers over man-made glass and carbon fibers are low cost, low density, comparable specific tensile properties, non-abrasive to the equipment, non-irritation to the skin, reduced energy consumption, less health risk, renewability, recyclability and bio-degradability. In order to gain the natural fiber reinforced plastic composites to be more and more acceptable in structural applications, applications of agricultural natural fibers and/or bio-based polymers are growing interest as the potential resources to replace a synthetic petroleum-based material [6-8].

Cellulose, which is the ubiquitous organic compound, is a structural component of the cell walls of many plants. Its industrial use is mainly for making paper and cardboard but recently it has also attracted significant interests for a source of biofuel production. A wide variety (non-wood and wood fibers) of natural fibers is represented schematically in Fig. 1-1.

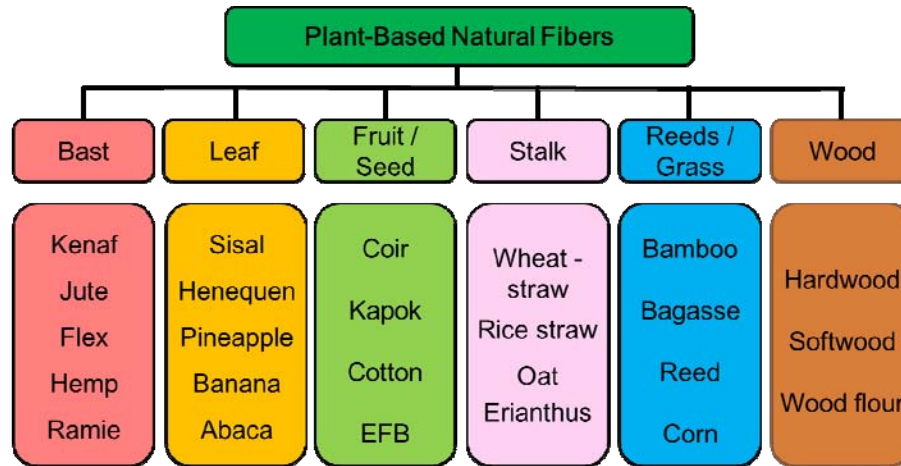


Figure 1-1. Classification of lignocellulosic natural fibers

Although natural fibers can offer the resulting composites many advantages, the usually polar fibers have inherently low compatibility with non-polar polymer matrices, especially hydrocarbon matrices such as polypropylene (PP) [9-11] and polyethylene (PE) [12-14]. The incompatibility may cause problems in the composite processing and material properties. Since the cellulose is hydrophilic property, natural fiber cannot be uniformly dispersed in most non-polar polymer media. This is a major disadvantage of natural fiber reinforced composites. Consequently, modification of natural fiber is important in order to improve compatibility with a wider variety of matrices.

Researchers are looking for the various possibilities of combining natural fibers such as sisal, flax, hemp, jute, banana, wood and various grasses with polymer matrices from non-renewable and renewable resources to have desirable performance for composite materials [15]. The field of natural fiber reinforced polymer composites promises to lead the environmental friendly system, high-potential natural fiber that can replace some of the synthetic materials.

1.4 Chemical surface modification

In order to improve the interfacial adhesion and dispersion between hydrophilic biomass filler and hydrophobic polymer matrix, many researcher in the field of natural fiber reinforced polymer composites particularly focused on the modification of natural fibers surface as fillers. This is a very important issue, because the simple addition of natural-organic fillers to a polymer matrix may lead to poor mechanical properties in comparison to the single polymer. Chemical modification such as acetylation, alkali, anhydride, silane, and isocyanate treatments is an interesting method to improve the surface properties of natural fibers, though having a primary drawback represented by the costs that, especially in the case of complicated techniques, can rise to such a level to make this method not suitable for industrial applications. Chemical and morphological modification can be very heterogeneous depending on the treatment conditions, therefore it is not easy to generalize.

Modification relies on chemical and physical techniques, mainly focused on grafting chemical groups capable of improving the interfacial interactions between fibers and polymer matrix. Promoters and compatibilizers in surface modification methods for the natural fiber reinforced polymer composites were described in many papers. Among different coupling agents, maleic anhydride is the most commonly used. In general, the literature reports improvements in tensile strength and elongation at break when maleic anhydride grafted matrix is used as compatibilizer (coupling agent) [16]. The most investigated matrices are polyolefin, while the adhesion promoters are mainly based on the same polyolefin or similar structure modified with maleic anhydride. However, the combination of promoters and compatibilizers between matrices and fibers is quite variable, depending on the polymer matrix used, the filler type and quantity, the adhesion promoter used (i.e. the polymer on which it is prepared, its molecular weight, the modifier percentage, etc.) and its amount, the

processing techniques, etc. In addition, chemical modifications and compatibilizer syntheses are relatively expensive, complicated, and time-consuming. A fundamental and complete solution to this problem requires an introduction of the new surface modification method.

1.5 Vapor-phase assisted surface polymerization (VASP) method

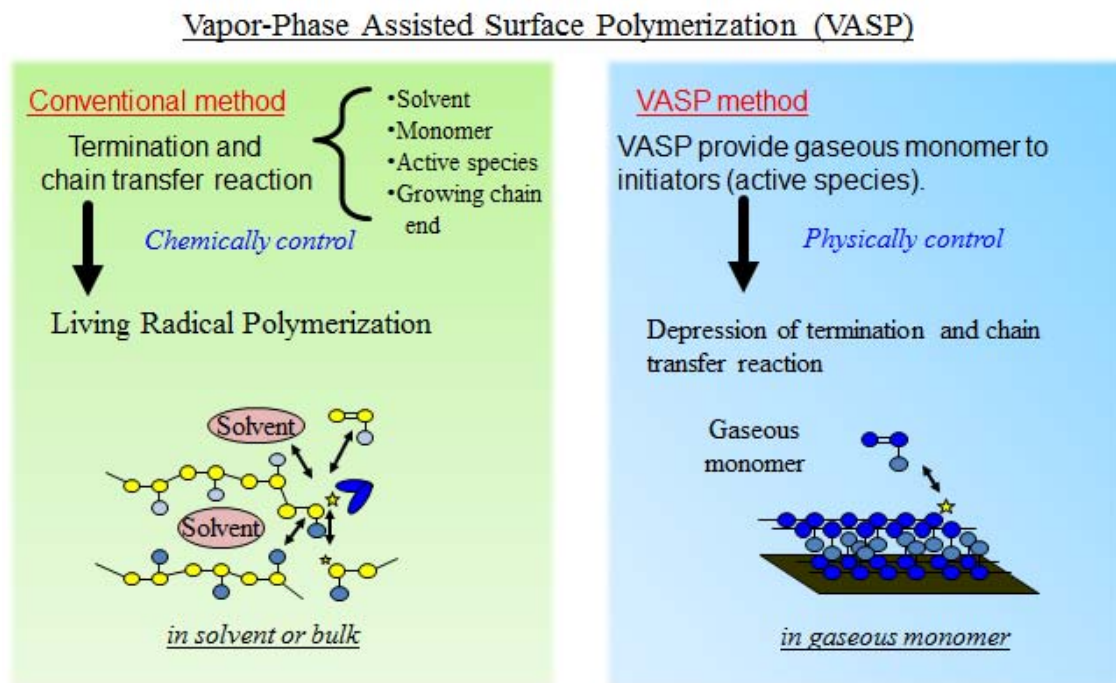
The coating method for the fine structures of complicated substrate surfaces with thin polymer layer is an excellent method, when their chemical properties are being modified. In order to overcome the problems associated with promoter and compatibilizers, I focused on the vapor-phase assisted surface polymerization (VASP) as a new surface modification method capable of improving the interfacial interactions between fibers and polymer matrix. Many technologies for the gaseous monomer processing of solid substrate surface have been developed, for chemical vapor deposition (CVD) [17-25], laser-generated gas-phase polymerization [26-28], and plasma polymerization [29-35]. Vapor processing is well suited to modify surface properties of bulk materials. However, these methods frequently make complex polymeric products such as insoluble networks. However, the VASP technique may give solutions for these problems, because of its solventless process and superior diffusing ability of gaseous monomers.

On the other hand, conventional technologies such as surface initiated polymerization (SIP) with free radicals [36-38], atom-transfer radical (ATRP), anion, iniferter polymerization methods, micro-contact printing with free radical polymerization, ring-opening metathesis polymerization (ROMP) [39-41] and “grafting on” the surface and photo lithography with free radical, they have allowed the design of fine patterns to be easily

reproduced on solid surfaces. In spite of the remarkable developments achieved in the techniques of polymer coating, there are still some problems associated with the liquid processes involved in polymer composite preparation, such as the requirement of a large amount of aqueous/organic solvent, the aggregation of substrates due to insufficient affinity with the monomer, the high viscosity of the monomer solution, the swelling of products in solution, volume shrinkage in the subsequent drying process, the difficulty of achieving monomer change and the lower level of homogeneous dispersibility in matrix polymers.

The VASP technique is the simplest method for coating thin layer on solid substrate surfaces with the advantages of being solvent-free and precise. It is unlike the plasma polymerization [42-48], initiators on substrate surfaces avoid unnecessary reactions in a gas phase and fabricate polymer layers with well-defined chemical structures that resemble their bulk counterparts. Gaseous and vaporized monomers have obvious advantages in their diffusion power onto various types of surfaces, such as extremely wide, very narrow spatial, complex 3D shaped, and even if chemically incompatible ones and VASP provide thin layer coatings on the surfaces, fulfill the narrow spaces of gaps and pores, and even confine particle substrates within capsules. This is because the VASP processes: adsorption of gaseous monomer molecules and simultaneous polymerization, are very gentle in comparison with liquid and melt processes. When these gaps and spaces are wider than the size of monomer molecule, the vaporized monomer can diffuse and penetrate interstitially give the additional advantages on within the solid substrates, and adsorb on surfaces by various forces such as H-bonding and hydrophobic interaction, or according to the adsorption equilibrium. After the diffusion and adsorption on the interstitial surfaces, the monomers polymerize in a manner of “pseudo-grafting from” form substrate surfaces. Polymer chains then grow on the surfaces of substrate by filling the spaces, giving a superior anchoring effect, with excellent

binding strength at the polymer/substrate interface.



Kim *et al.* described that VASP was applied to prepare biomass-based composites from wood flour and PLLA. VASP of LLA successfully proceeded on wood flour surfaces, which became covered by the accumulation of newly generated PLLA. Kim and co-authors focused on the interfacial interaction with substrate surfaces and the formation of highly crystallized polymer layers, which open up the possibility for the composite construction of specific surfaces and interfaces. There are some interactive effects between the wood flour surfaces and PLLA layers. To our knowledge, however, there is no previous report on the mechanical properties of fiber reinforced thermoplastic composites. Therefore, VASP is applied to one of very attractive surface modification method in polymer composite fields in this thesis.

1.6 Agricultural wastes

Agricultural residues are excellent alternative waste materials to substitute wood because they are plentiful, widespread, and easily available. Aside from their abundance and renewability, utilization of agricultural residues has advantages for economy, environment, and technology. Biomass waste such as agricultural residues is creating great environmental concerns, with approximately 200 billion tonnes of lignocellulosic wastes being produced annually [49]. Much effort has focused to find alternatives and environmental friendly handling and disposal of these wastes, it include recycling to produce revenue generating products. Although most biomass is suitable and is being converted to animal feed [50], there is still exploitation potential as agricultural residues are abundant, renewable, and relatively economical.

The scope of the work in natural fiber reinforced plastics field is to process agricultural waste fibers in order to evaluate and compare their suitability as reinforcing agents for composite applications. Although there are some useful studies in the literature on agricultural fibers in composites, there are still many gaps in information and the knowledge of composites including agriculture residues, which must be closed in order to stimulate commercial production of these novel materials.

1.7 Research targets

Herein, I focused on agricultural waste as an alternative material of petroleum-based material. Agricultural waste can be a valuable resource because of renewable material. In

order to provide a valuable greener product using agricultural waste, polymer/ agricultural waste composites has been fabricated in academic and industrial fields. Therefore, applications of agricultural natural fibers and/or bio-based polymers are proposed as the potential resources to replace a synthetic petroleum-based material. Since, however, the incompatibility between the hydrophilic natural fiber and hydrophobic polymer matrices makes it difficult to disperse the individual fiber throughout polymer matrices, and the incorporation of agricultural waste into polymer matrices may compromise certain mechanical properties. In order to overcome the poor compatibility between the natural fiber and polymer matrices, this thesis is studied and discussed in the control of surface property to induce original potentials of natural fiber in polymer/ agricultural waste composites.

This thesis consists of five chapters; Chapter 1 deals with an introduction of polymer composites reinforced with cellulose based on fibers for sustainable greener production and raise some issues for it. Chapter 2 deals with the enhancement of interface adhesion between polymer and natural fiber using compatibilizer. In order to evaluate mechanical properties of the compatibility between polypropylene (PP) and *Erianthus* fiber (ETF), maleic anhydride-modified polypropylene (MAPP) as a compatibilizer was applied to fabricate the composites. Chapter 3 deals with a simple surface modification method instead of using compatibilizer for the enhancement of compatibility between matrices and natural fibers. To overcome bothersome points in compatibilizer application, the author has been focusing on the vapor-phase assisted surface polymerization (VASP) that is not only a surface coating method for fabrication of composites but it will be also a wide range of applicable substrates. Chapter 4 deals with development of VASP method for practical use. As more simple and large scale of the coating method than previous one, the gas-flow type of vapor-phase assisted surface polymerization (VASP-F) was developed, and the substrate surface could be polymerized

through monomer mist produced by monomer bubbling. Chapter 5 conclude from my result that this study might be useful to the improvement of compatibility in the polymer/agricultural waste composites as a greener product for future environments.

1.8 Reference

- [1] A. Mohammad, “Barriers of commercial power generation using biomass gasification gas: A review”, *Renewable and Sustainable Energy Reviews*. (2013) 29, 201-215.
- [2] L. Montero de Espinosa, MAR. Meier, “Plant oils: The perfect renewable resource for polymer science”, *European Polymer Journal*. (2011) 47, 837-852.
- [3] J M. Raquez, M. Deléglise, M F. Lacrampe, P. Krawczak, “Thermosetting (bio)materials derived from renewable resources: A critical review”, *Prog Polym Sci*. (2010) 35, 487-509.
- [4] O. Faruk, A K. Bledzki, H-P Fink, M. Sain, “Biocomposites reinforced with natural fibers: 2000–2010”, *Progress in Polymer Science*. (2012) 37, 1552-1596.
- [5] C S. Wu, “Renewable resource-based composites of recycled natural fibers and maleated polylactide bioplastic: Characterization and biodegradability”, *Polym Degrad Stabil*. (2009) 94, 1076-1084.
- [6] S V. Joshi, L T. Drzal, A K. Mohanty, S. Arora, “Are natural fiber composites environmentally superior to glass fiber reinforced composites?”, *Composites: Part A*. (2004) 35, 371-376.
- [7] R S. Sinha, A K. Kundu, S. Maiti, “Polymers from renewable resources--13. Polymers from rosin acrylic acid adduct”, *Eur Polym J*. (1990) 26, 471-474.
- [8] B. Kamm, P R. Gruber, M. Kamm, “Biorefinery industrial processes and products, status and future direction”, *Vol. 1–2. Weinheim: Wiley-Verlag GmbH and Co KGaA*; (2006).
- [9] G. Cantero, A. Arbelaiz, R. Llano-Ponte, I. Mondragon, “Effects of fibre treatment on wettability and mechanical behaviour of flax/polypropylene composites”, *Compos Sci Technol*. (2003) 63, 1247-1254.
- [10] P. V. Joseph, G. Mathew, K. Joseph, G. Groeninckx, S. Thomas, “Dynamic mechanical

- properties of short sisal fibre reinforced polypropylene composites”, *Compos Part a-Appl S.* (2003) 34, 275-290.
- [11] A. K. Rana, A. Mandal, S. Bandyopadhyay, “Short jute fiber reinforced polypropylene composites: effect of compatibiliser, impact modifier and fiber loading”, *Compos Sci Technol.* (2003) 63, 801-806.
- [12] J. George, S. S. Bhagawan, N. Prabhakaran, S. Thomas, “Short Pineapple-Leaf-Fiber-Reinforced Low-Density Polyethylene Composites”, *J Appl Polym Sci.* (1995) 57, 843-854.
- [13] D. Kocak, M. Tasdemir, I. Usta, N. Merdan, M. Akalin, “Mechanical, thermal, and microstructure analysis of silk- and cotton-waste-fiber-reinforced high-density polyethylene composites”, *Polym-Plast Technol.* (2008) 47, 502-507.
- [14] C. Xion, R. R. Qi, W. J. Gong, “The preparation and properties of wood flour/high density polyethylene composites by in-situ reaction extrusion”, *Polym Advan Technol.* (2009) 20, 273-279.
- [15] A. K. Mohanty, L. T. Drzal, M. Misra “Engineered natural fiber reinforced polypropylene composites: Influence of surface modifications and novel powder impregnation processing”, *Journal of Adhesion Science and Technology.* (2002) 16, 999–1015.
- [16] B. S. Panigrahy, A. Rana, P. Chang, S. Panigrahi, “Overview of flax fiber reinforced thermoplastic composites”, *Can Biosyst Eng J.* (2006) 06–165:1–12.
- [17] C. J. Carmalt, E. S. Peters, S. J. King, J. D. Mileham, D. A. Tocher, “Molecular Design of Precursors for the Chemical Vapor Deposition of Group 13 Chalcogenides”, *Modern Aspects of Main Group Chemistry*, vol. 917: American Chemical Society. (2005) 917, 376-389.
- [18] A. W. Maverick, A. M. James, H. Fan, R. A. Isovitsch, M. P. Stewart, E. Azene, Z. T. Cygan “New Routes Toward Chemical and Photochemical Vapor Deposition of Copper Metal”, *Inorganic Materials Synthesis*, vol. 727: American Chemical Society. (1999) 100-112.
- [19] S. Kleckley, H. Wang, I. Oladeji, L. Chow, T. K. Daly, P. R. Buseck, T. Solouki, A. Marshall, “Fullerenes and Polymers Produced by the Chemical Vapor Deposition Method”, *Synthesis and Characterization of Advanced Materials*, vol. 681: American Chemical Society. (1997) 51-60.
- [20] K. A. Singmaster, F. A. Houle, “Laser-Assisted Chemical Vapor Deposition from the Metal Hexacarbonyls”, *Laser Chemistry of Organometallics*, vol. 530: American Chemical Society. (1993) 292-301.
- [21] M. Shirai, M. Tsunooka, “Surface-Imaging Resists Using Photogenerated Acid-

- Catalyzed SiO₂ Formation by Chemical Vapor Deposition”, *Polymers for Microelectronics*, vol. 537: American Chemical Society. (1993) 180-193.
- [22] L. M. Tonge, D. S. Richeson, T. J. Marks, J. Zhao, J. Zhang, B. W. Wessels, “Organometallic Chemical Vapor Deposition”, *Electron Transfer in Biology and the Solid State*, vol. 226: American Chemical Society. (1989) 351-368.
- [23] T. W. F. Russell, B. N. Baron, S. C. Jackson, R. E. Rocheleau, “Physical Vapor Deposition Reactors”, *Microelectronics Processing*, vol. 221: American Chemical Society. (1989) 171-198.
- [24] Jensen Klavs F. Chemical Vapor Deposition. *Microelectronics Processing*, vol. 221: American Chemical Society; 1989. p. 199-263.
- [25] K. F. Jensen, D. I. Fotiadis, D. R. McKenna, H. K. Moffat, “Growth of Compound Semiconductors and Superlattices by Organometallic Chemical Vapor Deposition”, *Supercomputer Research in Chemistry and Chemical Engineering*, vol. 353: American Chemical Society. (1987) 353-375.
- [26] J. Pola, “Laser-generated silenes and their gas-phase polymerization”, *Radiat Phys Chem.* (1997) 49, 151-154.
- [27] J. Pola, “Polycarbosilane-based coatings by laser-induced polymerization of silenes in the gas phase”, *Surface and Coatings Technology*. (1998) 100-101, 408-410.
- [28] D. Cukanová, J. Pola, “Efficient laser-induced generation and polymerization of the highly unsaturated compound diethynylsilene in the gas phase”, *J Organomet Chem.* (1993) 453, 17-20.
- [29] S. Zanini, C. Riccardi, M. Orlandi, C. Colombo, F. Croccolo, “Plasma-induced graft-polymerisation of ethylene glycol methacrylate phosphate on polyethylene films”, *Polym Degrad Stabil.* (2008) 93, 1158-1163.
- [30] A. A. Serrano, P. M. Monleón, J. L. Gómez Ribelles, “Plasma-induced polymerisation of hydrophilic coatings onto macroporous hydrophobic scaffolds”, *Polymer*. (2007) 48, 2071-2078.
- [31] S. K. Nema, P. M. Raole, S. Mukherjee, P. Kikani, P. I. John, “Plasma polymerization using a constricted anode plasma source”, *Surface and Coatings Technology*. (2004) 179, 193-200.
- [32] Z. G. Qiu, G. Y. Jing, Z. Z. Fa, W. D. Bao, “Experimental investigation of plasma dust and plasma polymerization”, *Surface and Coatings Technology*. (2000) 131, 525-527.
- [33] P. Spatenka, H. J. Endres, J. Krumeich, R. W. Cook, “Process control of plasma polymerization in a large industrial reactor”, *Surface and Coatings Technology*. (1999) 116-119, 1228-1232.

- [34] A. Tanioka, Y. Yokoyama, M. Higa, K. Miyasaka, "Membrane potential of bipolar membranes prepared by plasma-induced grafted polymerization on porous polyolefin", *Colloids and Surfaces B: Biointerfaces*. (1997) 9, 1-7.
- [35] H. Yasuda, M. Gazicki, "Biomedical applications of plasma polymerization and plasma treatment of polymer surfaces", *Biomaterials*. (1982) 3, 68-77.
- [36] P. Pasetto, Hln. Blas, F. Audouin, Cd. Boissière, Cm. Sanchez, M. Save, et al. "Mechanistic Insight into Surface-Initiated Polymerization of Methyl Methacrylate and Styrene via ATRP from Ordered Mesoporous Silica Particles", *Macromolecules*. (2009) 42, 5983-5995.
- [37] Q. Zhou, Y. Nakamura, S. Inaoka, M-k. Park, Y. Wang, X. Fan, et al. "Surface-Initiated Anionic Polymerization: Tethered Polymer Brushes on Silicate Flat Surfaces", *Polymer Nanocomposites*, vol. 804: American Chemical Society. (2001) 39-55.
- [38] R. Chen, S. Zhu, S. Maclaughlin, "Grafting Acrylic Polymers from Flat Nickel and Copper Surfaces by Surface-Initiated Atom Transfer Radical Polymerization", *Langmuir*. (2001) 24, 6889-6896.
- [39] D. A. Rankin, A. B. Lowe, "Synthesis of Polyelectrolytes via Ring Opening Metathesis Polymerization", *Polyelectrolytes and Polyzwitterions*, vol. 937: American Chemical Society. (2006) 117-128.
- [40] Y-D. Wu, Z-H. Peng, "Theoretical Study of the Mechanism and Stereochemistry of Molybdenum Alkylidene Catalyzed Ring-Opening Metathesis Polymerization", *Transition State Modeling for Catalysis*, vol. 721: American Chemical Society. (1999) 187-197.
- [41] R. H. Grubbs, C. B. Gorman, E. J. Ginsburg, J. W. Perry, S. R. Marder, "New Polymeric Materials with Cubic Optical Nonlinearities Derived from Ring-Opening Metathesis Polymerization", *Materials for Nonlinear Optics*, vol. 455: American Chemical Society. (1991) 672-682.
- [42] S. Zanini, C. Riccardi, M. Orlandi, C. Colombo, F. Croccolo, "Plasma-induced graft-polymerisation of ethylene glycol methacrylate phosphate on polyethylene films", *Polym Degrad Stabil*. (2008) 93, 1158-1163.
- [43] A. Serrano Aroca, M. Monleón Pradas, J L. Gómez Ribelles, "Plasma-induced polymerisation of hydrophilic coatings onto macroporous hydrophobic scaffolds", *Polymer*. (2007) 48, 2071-2078.
- [44] S K. Nema, R M. Raole, S. Mukherjee, P. Kikani, P I. John PI, "Plasma polymerization using a constricted anode plasma source", *Surface and Coatings Technology*. (2004) 179, 193-200.
- [45] Z G. Qiu, G Y. Jing, Z Z. Fa, W D. Bao, "Experimental investigation of plasma dust and

- plasma polymerization”, *Surface and Coatings Technology*. (2000) 131, 525-527.
- [46] P. Spatenka, H J. Endres, J. Krumeich, R W. Cook, “Process control of plasma polymerization in a large industrial reactor”, *Surface and Coatings Technology*. (1999) 116-119, 1228-1232.
- [47] A. Tanioka, Y. Yokoyama, M. Higa, K. Miyasaka, “Membrane potential of bipolar membranes prepared by plasma-induced grafted polymerization on porous polyolefin”, *Colloids and Surfaces B: Biointerfaces*. (1997) 9, 1-7.
- [48] H. Yasuda, M. Gazicki, “Biomedical applications of plasma polymerization and plasma treatment of polymer surfaces”, *Biomaterials*. (1982) 3, 68-77.
- [49] A. K. Mohanty, M. Misra, G. Hinrichsen, “Biofibres, biodegradable polymers and biocomposites: an overview”, *Macromol. Mater. Eng.* (2000), 276, 1–24.
- [50] N. Kasai, A. Murata, H. Inui, T. Sakamoto, R. I. Kahn, “Enzymatic high digestion of soybean milk residue (okara)”, *J. Agric. Food Chem.* (2004), 52, 5709–5716.

Chapter 2. Development of biocomposites containing *Erianthus Arundinaceus* as cellulose resource crops

2.1 Introduction

The biomass materials are expected to contribute a key role for the reduction in carbon dioxide which induce reducing or decreasing energy consumption and dependency on fossil energy. It is attracting attention as one of the measures for depletion of petroleum resources and prevention of global warming [1, 2]. A production of bio fuels derived from biomass not only shows an effect of low environmental load because of lower generating of greenhouse gas than gasoline, but is expected to create secondary effects such as positive utilization of farmland and forest, formation of sustainable society, and creation of new industry and employment. However, the use of biomass in preparation of green product such as biocomposites increases the amount of grain and causes people to worry about food supply [3]. Natural resources as non-grains for the natural additives require numerous advantages such as a low cost, low density, high toughness, acceptable specific strength properties, the ease of separation, and biodegradability.

Erianthus (*Erianthus Arundinaceus*) has attracted considerable interest for a cellulose based resource crop which can resolve this problem [4-6]. *Erianthus* is a large perennial plant which grows naturally in Thailand, and, as it is strong against diseases and insects, has a strong resistance to dryness and excessive humidity, and can be highly productive even in a

land unsuitable for farming, it is experimentally cultivated recently as the raw material for bio ethanol in domestic and is used for studies on bio-ethanol [7].

Since natural fiber reinforced polymer composites, as an important branch in the field of composite materials, the research fields in electronic appliances, automobile and construction have been attractive [8, 9]. Although natural fibers can offer the resulting composites many advantages such as abundance and therefore low cost, biodegradability, minimal health hazards, low density, desirable fiber aspect ratio, and relatively high tensile and flexural modulus, the usually polar fibers have inherently low compatibility with non-polar polymer matrices, especially hydrocarbon matrices such as polypropylene (PP) and polyethylene (PE).

The innovation in this work is the dispersion of *Erianthus* fibers (ETF) with compatibilizer in PP by extrusion, to produce a material with an improvement in mechanical properties. The aim is to provide a general-purpose material from biomass that does not compete with food as an alternate material from the petroleum base. Non-grain crops such as cellulose resources crops for bio fuels are also attractive materials as same as agricultural wastes because of non-food crops. Although researchers have focused on a cellulose resource crops for the biofuels resource, studies for a materials resource is few. Prior to use, the ETF, obtained from the stem, was milled and sieved to promote fibrillation and increase aspect ratio. The composites were prepared in a twin screw extruder to choose the processing method for a good dispersion of ETF. After determination of the processing conditions, the composites were characterized by FTIR, thermogravimetry, mechanical properties, and scanning electronic microscopy.

2.2 Experimental

2.2.1 Materials

The materials employed in this investigation were polypropylene (PP - YF6, PP Japan Polypropylene Corporation, Ltd., Japan) as the matrix and MA-g-PP (New Max-1010, Sanyo Chemical Industries, Ltd., Japan) as the compatibilizer. *Erianthus* (*Erianthus Arundinaceus*) fibers (ETF) was purchased from National Agriculture and Food Research Organization (NARO) in Japan and used as received.

2.2.2 Grinding process

Fig. 2-1 shows the stems of *Erianthus* and pulverized *Erianthus* fibers. Cut *Erianthus* fibers (4-5cm) were pulverized in twice by the pin mills (Pulverizer M-2 MILL Model Machine; NARA MACHINERY Co., Ltd, JAPAN) under 7000 rpm with a screen size (0.5 mm). The particles were sieved by sieving machine (AS-200 model machine; Retsch Co., Ltd, JAPAN) to separate fiber size 0 – 63, 63 – 106, 106 - 150 and 150 - 250 μm (Table 2-1). The *Erianthus* fibers (ETF) were dried in an oven at 80 °C for 48 h, and stored in polyethylene bags until use. The separated fibers were measured to calculate aspect ratio in 400 pieces of fibers, respectively (Table 2-1). The separated fibers observed thermal degradation behavior, respectively (Fig. 2-2).



Figure 2-1. Photo Images of *Erianthus* (a), *Erianthus* stem (b), and the grinded *Erianthus* fibers (c)

Table 2-1. Distribution volume of *Erianthus* fibers (ETF) after sieving

Sample.	<i>Erianthus</i> fibers (ETF)				
	0-63 μm	63~106 μm	106~150 μm	150~250 μm	250 μm <
Weight ratio (wt%)	15.4	11.9	13.8	41.0	18.0
Short width(μm)	16.0	50.6	66.4	95.6	-
Long width(μm)	43.8	179.9	248.5	366.7	-
Aspect ratio	2.7	3.5	3.7	3.8	-

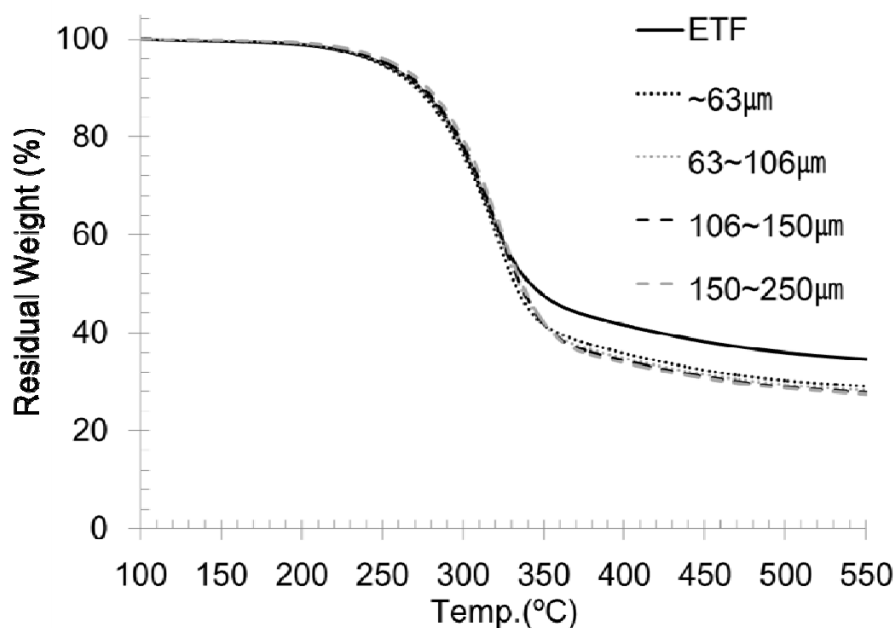


Figure 2-2. TG curves of differential size of *Erianthus* fibers (ETF)

2.2.3 Typical procedure of ETF/PP composites

30wt% of ETF and MAPP were compounded with PP using a small twin-screw extruder (160B Type, Imoto Machinery Co., Ltd, Japan). The mass ratio of MAPP to ETF was 0, 1, 3, 5, and 7wt%. The processing zone in extruder is divided into four temperature zones being individually adjustable. The temperature of each processing zone was maintained at 90-190-210-185 °C and the rotation speed was 16 rpm. After mixing of ETF and PP, the extrudate in the form of strands were allowed to cool to room temperature and pelletized using a pelletizer. The extruded pellets were stored in sealed polyethylene bags to avoid moisture infiltration.

2.2.4 Mechanical testing

The extruded pellets were injection molded for flexural test bars (20 mm x 5 mm x 2 mm) using an injection molding machine (IMC-18D1 , Imoto Machinery Co., Ltd, Japan) and the composite film (40 mm x 5 mm x 0.5 mm) for tensile test samples were prepared using a hot press machine(IMC-180C , Imoto Machinery Co., Ltd, Japan). The temperature, time, and pressure for hot-press process are 190 °C, 2 min, and 30 MPa, respectively. Flexural tests and tensile tests were conducted according to IMC-18E0 Model Machine (Imoto Machinery Co., Ltd, Japan) at a speed of 5 mm/min. The six replicates were prepared for these tests for each composite composition.

2.2.5 Characterization

Fourier transforms infrared (FTIR) spectra of WSFs and composites were recorded on a Perkin Elmer Spectrometer GX2000R. Reflection spectra were measured on a Golden Gate Diamond ATR (10500) module with a germanium crystal by the single-reflection ATR method. Sample sheets of equal size were soaked in water at 70°C for 24 h and air dried. The ratio of the weight of absorbed water in a swollen sample to the weight of the swollen sample refers to the equilibrium water content. Thermal degradation behavior of fibers and composites was analyzed by a thermogravimeter (TG). TG was conducted on a Seiko Instrumental Inc. EXSTAR 6200 TG/DTA system in an aluminum pan (5 mmφ) under a constant nitrogen flow (100 mL min⁻¹) using about 8-9 mg of film sample. Dynamic thermal degradation of the sample was conducted at prescribed heating rates, ϕ , of 10 °C min⁻¹ in a temperature range of 30 to 550 °C. The tensile fracture surface of composites sputtered carbon by a HITACHI E-1030 instrument and they were observed by a HITACHI- S3000N

scanning electron microscope (SEM) at an accelerating voltage of 4.3, 5.0, and 5.3kV.

2.3 Results and discussion

2.3.1 Pulverization of *Erianthus* fiber (ETF)

Fig. 2-3 shows the result of analyzing the composition of hemicellulose, cellulose, and lignin ingredients conducted by the method of Noor Ida *et al* [10-13]. As a result of the analysis not only on the composition of the entire stem but also on the inner stem and the rind, it is revealed that there is few lignin ingredient in the inner stem, of which the main ingredients are hemicellulose and cellulose [14]. Next, TG/DTG measurement was conducted in order to observe the thermal decomposition behavior of each sample (Fig. 2-4). While the weights of the stem and rind of *Erianthus* decreased at the temperature of 230 °C, the weight of the inside component is decreased at a lower temperature than that. It is supposed that thermal decomposition of hemicellulose ingredient, which is lower thermal degradation temperature, is suppressed by the rind which contains large quantity of lignin ingredient. Accordingly, we used the entire *Erianthus* stem as an organic filler to make polymer composites. Distribution of pulverized *Erianthus* powder separated to each fiber size by 0μm to 63μm, 63μm to 106μm, 106μm to 150μm and 150μm to 250μm, respectively.

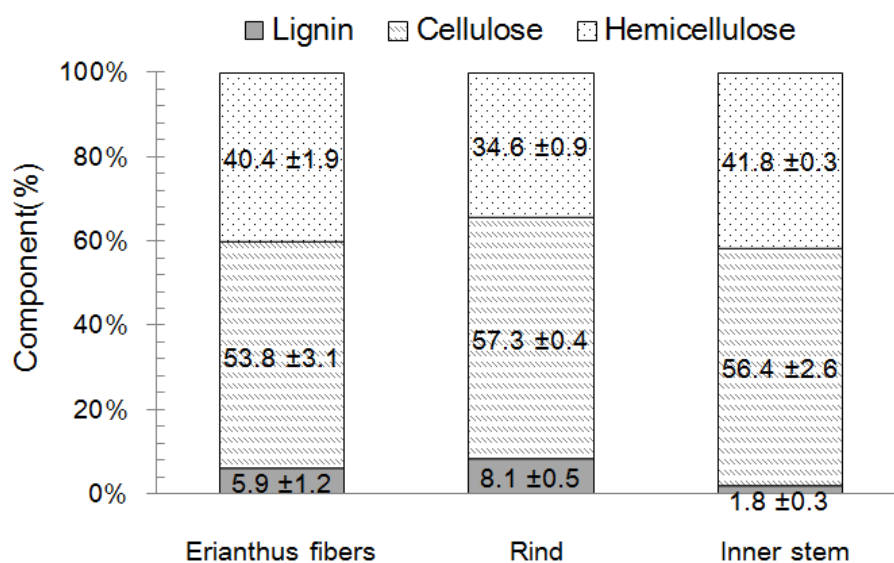


Figure 2-3. Chemical component of *Erianthus* fibers (ETF)

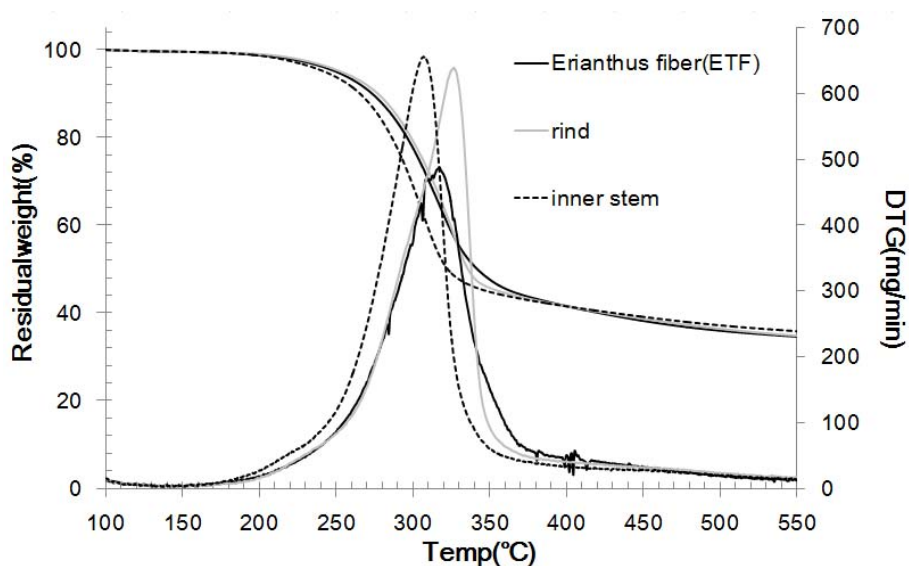


Figure 2-4. TG and DTG curves of *Erianthus*, rind, and inner stem

2.3.2 Mechanical Properties of ETF Composites

The quality of interfacial bonding is determined by several factors, such as the nature of fiber and polymer components, the fiber aspect ratio, the processing procedure and surface property. The short ETF and PP were mixed using the twin screw extruder as listed in Table 2-2, and the composites were pelletized. The test pieces for tensile and flexural test were molded from the composites. In order to investigate the effect of aspect ratio in ETF, PP composites containing each classified ETF were characterized by tensile tests (Fig. 2-5(a)). All of PP/ETF composites appeared to have lower tensile strength than PP as a matrix, and the tensile modulus were slightly higher than PP. This is due to lack of significant interfacial interaction between fillers and polymer matrix [15-18]. Above all, the composite containing ETF powder by 150 μ m to 250 μ m indicated higher tensile strength and lower tensile modulus in comparison with others. Due to the larger surface area in high aspect ratio of ETF, it was expected to high interact between fiber and matrix. And also, water absorption rate in PP/ETF composites was investigated, respectively. As a result, absorption rate of PP/ETF composite was increased with decrease of ETF size because surface area of ETF was increased in the matrix. Herein, the tensile fracture surface of composites was observed by SEM (Fig. 2-6(a-d)). As a result, the cross-section of the composite specimen using the classified fibers oriented to the injection direction. The gaps were easily found at interfaces because of weak interaction between small fibers and the PLLA matrix. Since the interaction at interfaces was increased with increasing of fiber surface area in matrix, the fractured fiber was observed in PP composite containing large ETF by SEM.

Table 2-2. Characteristics of PP/ETF composites

Entry.	Fibers Size	PP (wt.%)	ETF (wt.%)	Td10 (°C)	Water Absorbent (%)
1	—	100	0	401.3	0
2	0~63 μ m	70	30	300.7	6.2
3	63~106 μ m	70	30	307.8	5.6
4	106~150 μ m	70	30	310.5	4.9
5	150~250 μ m	70	30	320.6	4.1

The flexural test performed according to three points of the bending test according to JIS K 7171, and the PP/ETF samples evaluated flexural strength and modulus respectively. From the results as shown in Fig. 2-5(b), unlike the results of tensile test in PP/ETF composites, the results of the flexural strength and modulus were higher than PP. ETF has higher flexural modulus than PP, it is contributed to compressive strength because flexural strength contributed to both tensile and compression. Since ETF works as the filler in polymer matrix, the larger classified fiber has its tendency.

Since ETF as a cellulose resource crop is hydrophilicity and PP is hydrophobicity, they are immiscible materials, respectively. The interface adhesion between fibers and polymer matrix in fiber reinforced plastics is significantly influenced on the mechanical properties. To obtain the compatibility between ETF and PP, maleic anhydride modified polypropylene (MAPP) as a compatibilizer was used for the composite to evaluate the mechanical properties [19]. ETF classified by the 106-150 μ m and 150-250 μ m of sieves showed the higher mechanical performances in composite without a compatibilizer. It was not only mixed in PP under weight ratio of 30/70 (wt/wt), but also added MAPP 1, 3, 5 and 7% to make the ETF/PP/MAPP pellet using extruder (Table 2-3). The results of tensile strength and modulus were shown in Fig. 2-7(a).

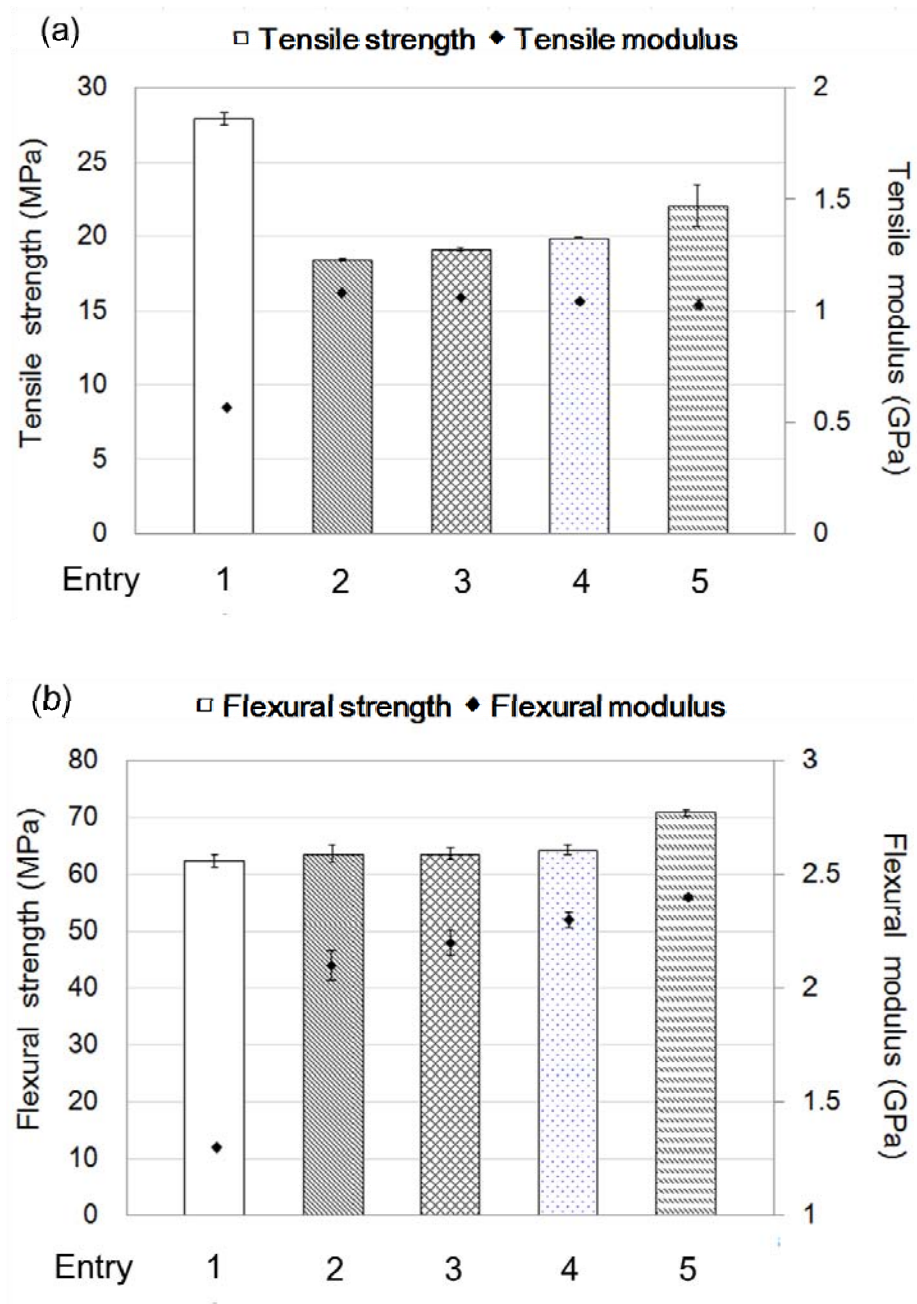


Figure 2-5. Effect of size distribution of fiber on the ETF/PP composites tensile strength and modulus (a), flexural strength and modulus (b)

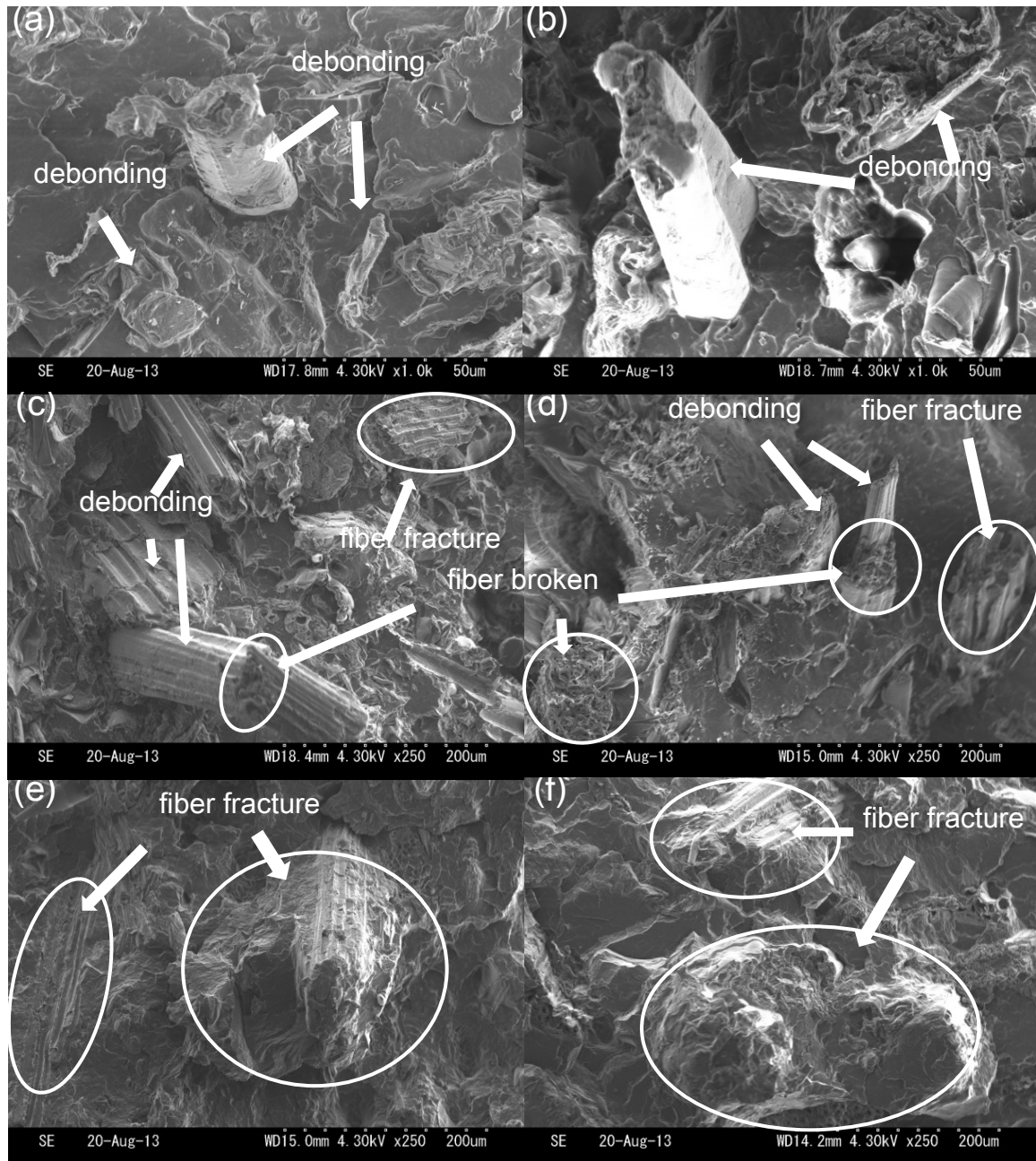


Figure 2-6. Cross-section (Vertical direction is injection direction) images of PP/ETF and PP/ETF/MAPP composites using SEM: Entry 2(a), Entry 3(b), Entry 4(c), Entry 5(d), Entry 4-5(e), and Entry 5-3(f)

As a whole, The PP/ETF composite including MAPP shows higher performances for the tensile strength and modulus in comparison with the PP/ETF composite without the

compatibilizer [20]. It is supposed that the interface adhesion between ETF and PP matrix was improved using MAPP as a compatibilizer. Since the PP/ETF/MAPP composite shows lower value of water absorption than the PP/ETF composite, it is indicated that MAPP in the PP/ETF/MAPP composite was smoothly reacted on ETF surface [21, 22]. Although the flexural strength and modulus in PP/ETF composites were increased with 1, 3, 5wt% of MAPP in the case of ETF powder classified with 106-150 μ m sieve used, the flexural strength and modulus in PP/ETF composites including 7wt% of MAPP was decreased. On the other hand, the tensile strength and modulus of composite including the ETF classified at 150-250 μ m were increased with the addition of 1wt% and 3 wt% of MAPP, but the products including 5wt% and 7wt% of MAPP indicated the lower tensile strength and modulus. In the results of flexural strength and modulus in the composite including MAPP, the mechanical properties increased in comparison with PP/ETF composite with no addition of MAPP (Fig.2-7(b)). In addition, addition effects of MAPP differ depending of ETF fiber size as similar to the results of tensile test. In case of the ETF fiber classified at 106-150 μ m, the composite including 5wt% MAPP showed the highest flexural strength and modulus, which were approximately 1.3 times higher than non-additive. On the other hand, the addition of 3wt% MAPP to the composite including ETF classified at 150-250 μ m showed the highest flexural strength and modulus. Therefore, the additive effect of MAPP is different according to the filled ETF size in the composite. To give significantly effect to the interface adhesive between ETF and polymer by the compatibilizer, the mechanical properties in the resulting products were affected. As a reference test, the flexural strength and modulus of PP were measured after addition of only 5wt% MAPP. It was indicated that the flexural strength of PP/5wt%MAPP was 57.0MPa and modulus was 1.13GPa. The resulting of these mechanical properties was decreased around 10-13% in comparison with that of PP. The fiber in the polymer induced reinforcement effect causing to affect the mechanical properties. And also,

the mechanical properties of the composite might be decreased by the excess addition of MAPP to the PP. The effect of MAPP depended on the surface area of ETF fiber. The mechanical properties indicated the decreasing tendency when the addition of MAPP exceeded a threshold because the mechanical strength of MAPP oneself is not so high.

Table 2-3. Characteristics of PP/ETF/MAPP composites

Entry.	Fibers Size	PP (wt.%)	ETF (wt.%)	MAPP (wt.%)	Water Absorbent (%)
4-1	106~150 μ m	70	30	100 : 1	3.7
4-3	106~150 μ m	70	30	100 : 3	3.5
4-5	106~150 μ m	70	30	100 : 5	3.3
4-7	106~150 μ m	70	30	100 : 7	3.1
5-1	150~250 μ m	70	30	100 : 1	3.4
5-3	150~250 μ m	70	30	100 : 3	3.0
5-5	150~250 μ m	70	30	100 : 5	2.8
5-7	150~250 μ m	70	30	100 : 7	2.6

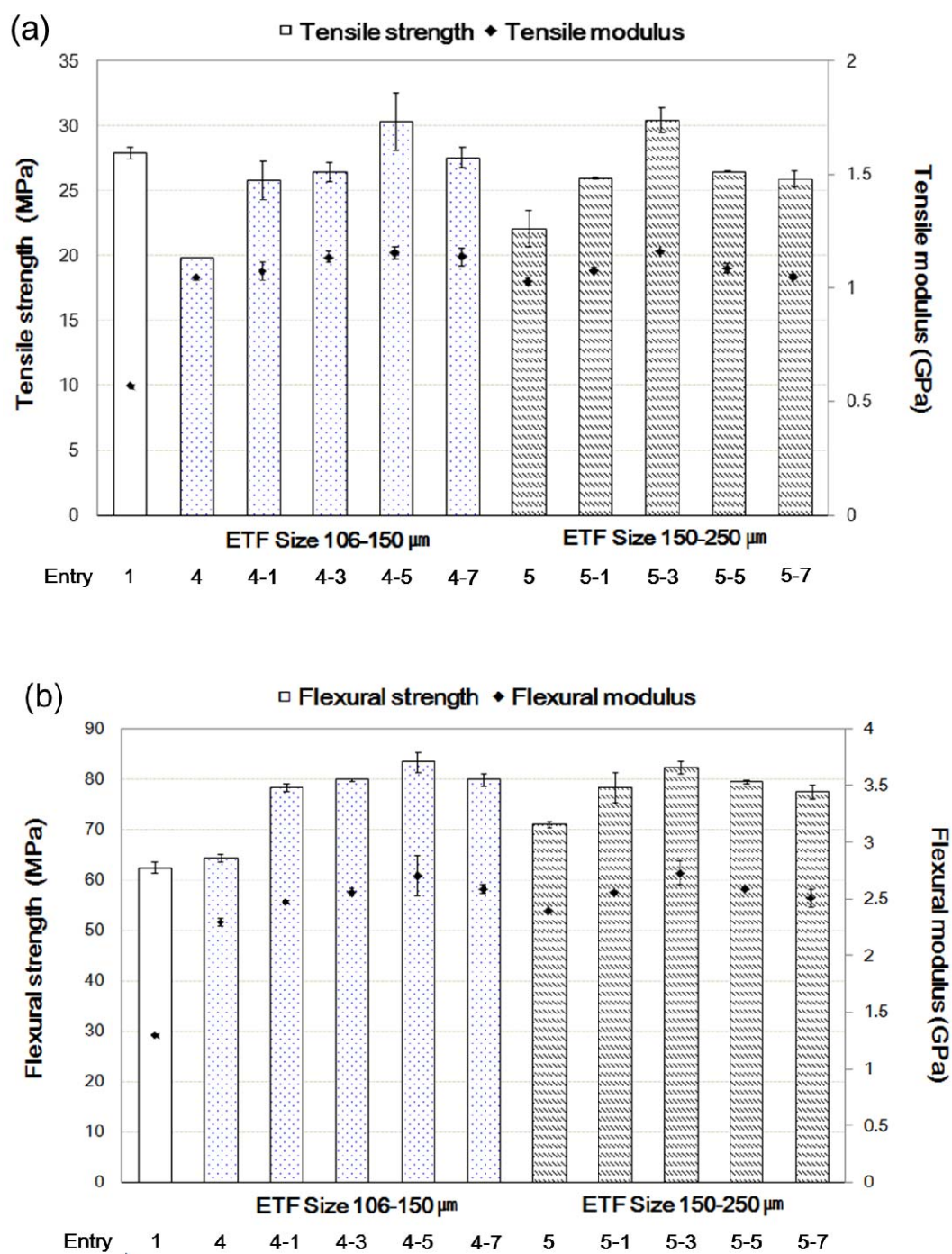


Figure 2-7. Influence of MAPP to ETF/PP composites tensile strength and modulus (a), flexural strength and modulus (b)

The specimen provided through injection mold was fractured perpendicularly to an injection direction and observed in a direction perpendicular to the specimen surface with a scanning electron microscope. The SEM images as shown in Figure 2-6(e-f) didn't show the interface destruction between polymer matrix and fiber, which unlike the case of the ETF/PP composites it showed the destruction of the fiber mainly [23]. Therefore, it was clear that the interface adhesion between polymer matrix and fiber in ETF/PP/MAPP composite was increased by addition of MAPP in comparison with the ETF/PP composite.

2.3.3 Thermal properties of composites

The thermal degradation behavior of ETF/PP composites was observed by TG, respectively. The ETF/PP composite showed two-step degradation behavior in comparison with that of ETF or PP as shown in Fig.8. It was found that the composite including larger size of fiber had slightly higher the heat resistance than that including smaller size of fiber. It is supposed that the degradation of ETF/PP composite first showed thermal degradation of fiber in the composite then degradation of PP component occurred continuously. The fiber size of ETF in the composite did not show significant difference of the thermal degradation behavior of fiber in itself. Therefore, in order to accelerate the thermal degradation at the contact point of fiber in the polymer because fiber dispersing in the polymer works like a wedge for molecules chain, the thermal degradation of composite including smaller size of fiber might be slightly accelerated in comparison with larger size of fiber. Since the smaller size of fiber in the composite has larger contact area with polymer matrix, the ETF fiber in ETF/PP composite was easily degraded. On the other hand, the thermal degradation behavior of ETF/PP/ MAPP composite showed no significant differences when it compared with that of composite under additive free. Addition of MAPP in the composite didn't affect the

degradation behavior of the composite because the quantity of MAPP was very few in a whole.

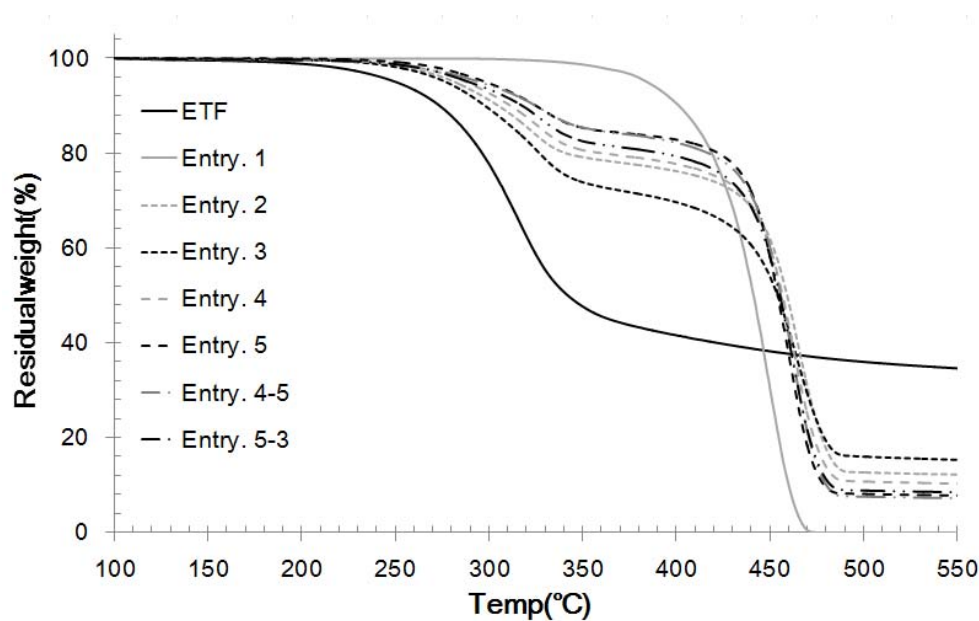


Figure 2-8. TG curves of PP, ETF, ETF/PP composites, and ETF/PP/MAPP

2.4 Conclusion

The PP composite with *Erinathus* as a cellulose resource crops was successfully prepared using twin screw extrusion followed by injection molding, and the influence of the sieved fiber and compatibilizer were examined to give the mechanical properties of the ETF/PP composite. As results of the tensile test and the flexural test, even though mechanical properties of PP were decreased by addition of ETF as filler, ETF/PP composite improved the interface adhesion between polymer matrix and fiber by addition of compatibilizer and mechanical properties also improved. The classified fiber according to sieve size shows difference in contact area of the fiber in the polymer matrix, the resulting product was influenced to the thermal degradability of the composite, and it not affected only the

mechanical properties of the composite but also the amount of compatibilizer in the matrix. In this result, it is the first report that the polymer composite using *Erianthus*, which is not only cellulose resource crops but also one of agricultural wastes, was prepared and evaluated, and also ETF can greatly expect its potential as a filler through further investigation for natural fiber reinforced composites.

2.5 Reference

- [1] A. Mohammad, “Barriers of commercial power generation using biomass gasification gas: A review”, *Renewable and Sustainable Energy Reviews*. (2013) 29, 201-215.
- [2] A K. Mohanty, M Misra, L T. Drzal, “Sustainable biocomposites from renewable resources: opportunities and challenges in the green materials world”, *J Polym Environ*. (2002) 10, 19-26.
- [3] K. Tokuyasu, “Development of small-scale bio-ethanol production system for domestic regional activation - Expectations for energy crops as raw materials developed-“, *Journal of the Japan Institute of Energy*. (2013) 92, 599-604.
- [4] S. Morita, N. Sekiya, J. Abe, “Impact of non-conventional natural gas”, *Journal of the Japan Institute of Energy*. (2013) 92, 562-563.
- [5] K. Ra, F. Shiotsu, J. Abe, and S. Morita, “Biomass yield and nitrogen use efficiency of cellulosic energy crops for ethanol production”, *Biomass and bioenergy*. (2012) 37, 330-334.
- [6] S. Irei, S. Fukuhara, Y. Terajima, T. Sakaigaichi, M. Matsuoka, A. Sugimoto, “Exploration and Collection of Sugarcane Wild Species (*Erianthus* spp.) in Okinawa Island”, *Uesagu report* (2008) 24, 47-53.
- [7] E. Morita, H. Mihasi, M. Sugihara, “Development of bio-ethanol integrated manufacturing technology using cellulose resources crop”, *Journal of the Japan Institute of Energy*. (2013) 92, 590-598.
- [8] M. Serizawa, K. Inoue, M. Ichi, “Development of kenaf fiber addition polylactic acid for electronic equipment”, *Polymer Society of Japan*. (2005) 62, 177-182.

- [9] C. Nyambo, A.K. Mohanty, M. Misra, "Polylactide-Based Renewable Green Composites from Agricultural Residues and Their Hybrids", *Biomacromolecules*. (2010) 11, 1654-1660.
- [10] N I. Nordin, H. Ariffin, Y. Andou, M A. Hassan, Y. Shirai, H. Nishida, W M Z. Wan Yunus, S. Karuppuchamy, N A. Ibrahim, "Modification of Oil Palm Mesocarp Fiber Characteristics Using Superheated Steam Treatment", *Molecules*, (2013) 18, 9132-9146.
- [11] N. Reddy, Y. Yang, "Properties of High-Quality Long Natural Cellulose Fibers from Rice Straw", *J. Agric. Food Chem.* (2006) 54, 8077-8081.
- [12] A K. Mohanty, M. Misra, G. Hinrichsen, "Biofibres, biodegradable polymers and biocomposites: An overview", *Macromol. Mater. Eng.* (2000) 277, 1-24.
- [13] R C. Sun, X F. Sun, X H. Ma, "Effect of ultrasound on the structural and physiochemical properties of organosolv soluble hemicelluloses from wheat straw", *Ultrasonics Sonochemistry*. (2002) 9, 95-101.
- [14] Y. Horikawa, T. Imai, R. Takada, T. Watanabe, K. Takabe, Y. Kobayashi, J. Sugiyama, "Chemometric Analysis with Near-Infrared Spectroscopy for Chemically Pretreated Erianthus toward Efficient Bioethanol Production", *Appl Biochem Biotechnol.* (2012) 166, 711-721.
- [15] F G. Torres, M L. Cubillas, "Study of the interfacial properties of natural fibre reinforced polyethylene", *Polymer Testing*. (2005) 24, 694-698.
- [16] F M B. Coutinho, T H S. Costa, "Performance of polypropylene-wood fiber composites", *Polymer Testing*. (1999) 18, 581-587.
- [17] M. Zampaloni, F. Pourboghra, S A. Yankovich, B N. Rodgers, J. Moore, L T. Drzal, A K. Mohanty, M. Misra, "Kenaf natural fiber reinforced polypropylene composites: A discussion on manufacturing problems and solutions", *Composites: Part A*. (2007) 38, 1569-1580.
- [18] K. Oksman, M. Skrifvars, J-F. Selin, "Natural fibres as reinforcement in polylactic acid (PLA) composites", *Composites Science and Technology*. (2003) 63, 1317-1324.
- [19] B. Kord, "Influence of Maleic Anhydride on the Flexural, Tensile and Impact Characteristics of Sawdust Flour Reinforced Polypropylene Composite", *World Applied Sciences Journal*. (2011) 12, 1014-1016.
- [20] C S. Wu, "Characterization of cellulose acetate-reinforced aliphatic-aromatic copolyester composites", *Carbohydrate Polymers*, (2012) 87, 1249-1256.
- [21] C. Nyambo, A K. Mohanty, M. Misra, "Effect of Maleated Compatibilizer on Performance of PLA/Wheat Straw-Based Green Composites", *Macromol. Mater. Eng.* (2011) 296, 710-718.

- [22] S J. Kim, J B. Moon, G H. Kim, C S. Ha, “Mechanical properties of polypropylene / natural fiber composites: Comparison of wood fiber and cotton fiber”, *Polymer Testing*. (2008) 27, 801-806.
- [23] N. Sombatsompop, C. Yotinwattanakumtorn, C. Thongpin, “Influence of Type and Concentration of Maleic Anhydride Grafted Polypropylene and Impact Modifiers on Mechanical Properties of PP/Wood Sawdust Composites”, *Journal of Applied Polymer Science*. (2005) 97, 475-484.

Chapter 3. Enhancement of compatibility based on vapor-phase assisted surface polymerization (VASP) method for poly (L,L-lactide) composites with wheat straw fiber

3.1 Introduction

In previous Chapter 2, ETF/PP composite materials were produced through composites of *Erianthus*, a cellulose resource crop, and PP by way of melting and injection molding, and the effect of the fiber size and addition of compatibilizer on the mechanical properties of the composites was reviewed. However, MAPP should be grafted in polymer, and the pre-test is required. And the can cause problems of environmental pollution and reduction in molecular weight. So focused on Vapor-phase Assisted Surface Polymerization (VASP)-treatment [1-3] as a modification method for the fiber surface and investigated. In addition, low environmental load / biodegradable polymer used in consideration of the composites were replaced with a PLLA [4-6]. Agricultural wastes can be used as filler materials in the poly (L,L-lactide) [PLLA] matrix as a bio-plastic to construct an all bio-based composite, it can be expected to enhance the mechanical property and to reduce costs. Previous investigations of biodegradable PLLA composites based on agricultural wastes have attempted to improve the interfacial adhesion between natural fibers and hydrophobic matrices [7-11]. In order to improve the compatibility between polymer matrices and agricultural waste in bio-based composite, I newly focus on vapor-phase assisted surface polymerization (VASP) technique that is the simplest method for coating thin layer on solid substrate surfaces with the advantages of being solvent less and precise [12]. After the diffusion and adsorption on the surfaces, the monomers polymerize on the substrate surfaces. VASP is an excellent method

for preserving the fine structures of delicate substrate surfaces such as biomaterials in comparison with liquid and melting processes.

Also, I have a new agricultural waste [13] used as a filler material was examined. The *Erianthus* fibers (ETF) in Chapter 2 was used as a filler material on the bio-ethanol is used as a study, but there are difficulties in use in the domestic, especially in Thailand and Malaysia country is cultivated mainly because a small amount. Due to these problems, a new cellulose-based resource crop by was reviewed. The standard of review (1) widely cultivated, (2) Annually restoration, (3) low price, (4) in conjunction with economic and other industries. I examined four kinds of focus in conformity. Among them were examined on agricultural waste. Agricultural wastes are an available of estimated 500 million tons in North America alone each year. Approximately 120 million tons of these residues are generated by wheat crops [14]. Only a small percentage is being used in applications such as feedstock and energy production. Most burn out in the field. So I'm are agricultural waste was used for this study.

The purpose of this paper is to present high-performance bio- based composite designed with VASP attributes. VASP of methyl methacrylate (MMA) was carried out on surfaces of WSF [15-20] as an agricultural waste to include in PLLA, which was expected to achieve improved mechanical properties in the composites. PMMA should be more compatible than WSF with PLLA because of the compatible in PLLA. PMMA was chosen here to modify compatible properties between the hydrophilic WSF and hydrophobic PLLA because PMMA is a hydrophobic polymer that adsorbed and coated on WSF. To evaluate VASP of MMA on WSF surface and the modified effect of VASP of PLLA / WSF composites, obtained composites were examined using various analytical methods.

3.2 Experimental

3.2.1 Materials

Monomer: MMA (Wako Pure Chemical Industries, Ltd.) was distilled under reduced pressure from CaH_2 just before polymerization. Substrate: wheat straw fibers (WSF) was purchased from National Agriculture and Food Research Organization (NARO) in Japan and used as received. Initiator: 2,2'-azobis(isobutyronitrile), (AIBN) was purchased from Wako Pure Chemical Industries, Ltd. and used as received. Polymer matrix: poly(L,L-lactide), PLLA was received from TOYOTA Ltd. All solvents were commercially obtained and used as received.

3.2.2 Grinding process

Cut wheat straw (4-5cm) was pulverized in twice by the pin mills (Pulverizer M-2 MILL Model Machine; NARA MACHINERY Co., Ltd, JAPAN) under 8000 rpm with a screen size (0.5 mm). The particles were sieved by sieving machine (AS-200 model machine; Retsch Co., Ltd, JAPAN) to choose fiber size 106-63 μm . The wheat straw fibers (WSF) were dried in an oven at 80 °C for 48 h, and stored in polyethylene bags until use.

3.2.3 Typical procedure of vapor-phase assisted surface polymerization (VASP)

AIBN adsorbed WSF was prepared in a similar manner as reported elsewhere in detail [3, 21-23]. Before VASP, to adsorb the initiator AIBN on the WSF surface, WSF (ca. 15 g)

was treated with a 0.25 mM CH₂Cl₂ solution (50 mL) of AIBN at a 1/100 weight ratio to WSF at 25 °C for 0.5 h under stirring. After the treatment, CH₂Cl₂ was removed under vacuum at room temperature, resulting in the production of powdery WSF. A typical procedure of VASP was carried out in an H-shaped glass tube reactor with a vacuum cock. The initiator-adsorbed WSF (ca. 15g) was put into a Petri dish (bottom surface area: 95.03 cm²) and the Petri dish was set in the bottom of one of the legs of the H-shaped glass tube reactor. 5.0 mL of MMA and 4-*tert*-butylcatechol (ca. 50 mg) were added in another bottom of the H-shaped glass tube. The reactor was degassed by three freeze-pump-thaw cycles and then sealed under a saturated atmosphere of vaporized MMA. Polymerization was carried out at 80 °C for 3 h under a saturated vapor pressure of $3.8 \pm 0.3 \times 10^3$ Pa in a thermostated oven. After VASP, obtained product was dried to remove adsorbed unreactant in vacuo and weighed to yield the PMMA/VWSF composites (treated with VASP in WSF). The product was analyzed intact with Fourier transform infrared (FTIR) spectroscopy, scanning electron microscopy (SEM), and thermogravimetry (TG). Free-polymers on VWSF particle were extracted using CHCl₃ with a Soxhlet apparatus for 24 h. The isolated polymers were dried and analyzed by FTIR, thermogravimetry (TG) and size-exclusion chromatography (SEC).

3.2.4 Typical procedure of WS/PLLA composite

WSF before and after VASP of MMA were compounded with PLLA using a small twin-screw extruder (160B Type, Imoto Machinery Co., Ltd, Japan). The mass ratio of the fiber to polymer was 5, 15, and 30 wt%. The processing zone in extruder is divided into four temperature zones being individually adjustable. The temperature of each processing zone was maintained at 90-180-195-175 °C and the rotation speed was 16 rpm. After mixing of WSF and PLLA, the extrudate in the form of strands were allowed to cool to room

temperature and pelletized using a pelletizer. The extruded pellets were stored in sealed polyethylene bags to avoid moisture infiltration.

3.2.5 Mechanical testing

The extruded pellets were injection molded for flexural test bars using an injection molding machine (IMC-18D1 , Imoto Machinery Co., Ltd, Japan) and the composite film for tensile test samples were prepared using a hot press machine(IMC-180C , Imoto Machinery Co., Ltd, Japan). Flexural tests and tensile tests were conducted according to IMC-18E0 Model Machine (Imoto Machinery Co., Ltd, Japan) at a speed of 5 mm/min. The six replicates were prepared for these tests for each composite composition.

3.2.6 Characterization

Fourier transforms infrared (FTIR) spectra of WSFs and composites were recorded on a Perkin Elmer Spectrometer GX2000R. Reflection spectra were measured on a Golden Gate Diamond ATR (10500) module with a germanium crystal by the single-reflection ATR method. Molecular weights of the sample were measured by size exclusion chromatography (SEC) on a TOSOH HLC-8320 SEC system with a refractive index (RI) detector at 40 °C using a TOSOH TSKgel Super HM-M column and chloroform (HPLC grade) eluent (0.6 mL min⁻¹). The calibration curves for SEC analysis were obtained using polystyrene standards with a low polydispersity (5.0×10^2 , $1.0^5 \times 10^3$, 2.5×10^3 , 5.87×10^3 , 9.49×10^3 , 1.71×10^4 , 3.72×10^4 , 9.89×10^4 , 1.89×10^5 , 3.97×10^5 , 7.07×10^5 , 1.11×10^6 , TOSOH Corporation).

The sample (12 mg) was dissolved in chloroform (2 mL) and the solution was filtered through a membrane filter with a 0.45 μm pore size.

Thermal degradation behavior of PLLA/VWSF and PLLA/WSF composites was analyzed by a thermogravimeter (TG). TG was conducted on a Seiko Instrumental Inc. EXSTAR 6200 TG/DTA system in an aluminum pan (5 mm ϕ) under a constant nitrogen flow (100 mL min⁻¹) using about 8-9 mg of film sample. Dynamic thermal degradation of the sample was conducted at prescribed heating rates, ϕ , of 10 $^{\circ}\text{C min}^{-1}$ in a temperature range of 30 to 550 $^{\circ}\text{C}$. WSF samples before and after VASP of MMA and the tensile fracture surface of composites sputtered carbon by a HITACHI E-1030 instrument and they were observed by a HITACHI- S3000N scanning electron microscope (SEM) at an accelerating voltage of 4.3, 5.0, and 5.3kV.

3.3 Results and discussion

3.3.1 VASP of MMA on wheat straw fibers (WSF)

Performances of composite rely on the dispersibility of biomass fiber in polymer matrix. One of the advantages of vapor-phase assisted surface polymerization (VASP) process to natural fibers is to be able to cover the substrate surface by the accumulation of the anew generated polymer [3]. Poly methyl methacrylate (PMMA) shows good affinity to PLLA [24]. To investigate the properties of the PLLA composite containing WSF, the surface modification of WSF was conducted using VASP of methyl methacrylate (MMA). In this report, we attempted to prepare PLLA composites with WSF which was coated by VASP of

MMA in order to obtain high performance of biomass based composites. VASP of MMA was carried out on WSF as a substrate, on which used AIBN as a well-known initiator for the radical polymerization of MMA [12]. The polymerization was conducted under saturated vapor pressure of MMA at 80 °C as listed in Table 3-1. The products were analyzed by FT-IR, SEM, TG, and SEC.

Table 3-1. VASP of methyl methacrylate (MMA) with AIBN on wheat straw fibers (WSF)

Entry	WSF		MMA (mL)	Time (h)	Temp (°C)	Increment		M_w ($\times 10^4$)	M_w/M_n
	g	AIBN ^{a)} (mg/g)				g	wt (%)		
A	51.8	51.6	25.9	3	80	77.3 \pm 1.1	48.8 \pm 0.9	45.5	3.7

a) AIBN: 2,2'-Azobis(isobutyronitrile)

As a result, weight of WSF after VASP of MMA for 3h was increased around 47-50 wt%. The WSF after VASP of MMA was washed by CHCl_3 through Soxhlet extraction to measure the molecular weight of PMMA. SEC result of extracted PMMA shows $M_w = 45.5 \times 10^4$ and $M_w/M_n = 3.7$.

In Fig. 3-1, FTIR spectra of WSF before and after VASP of MMA were observed as shown in Fig. 3-1. And also commercial available PMMA was measured as reference. WSF after VASP of MMA showed the characteristic peaks at 1721 cm^{-1} assignable to $\nu_{\text{C=O}}$ as same as a standard PMMA. The FTIR spectrum of VASP of PMMA on VWSF shows no peak in the wavenumber range of $3100\text{-}3700 \text{ cm}^{-1}$ assignable to $\nu_{\text{O-H}}$ of hydroxyl groups in original WSF, indicating that the surfaces were covered by PMMA. The signal at 1730 cm^{-1} for carbonyl stretching bond in WSF is attributed to hemicellulose [25, 26]. When the

accumulated PMMA layers were removed using CHCl_3 with a Soxhlet extraction apparatus, the residual WSF ingredient showed almost the same FT-IR spectrum as the original WSF. Interestingly, the $\nu_{\text{C=O}}$ absorption peak on residual VWSF surfaces after the extraction treatment also appeared at 1721 cm^{-1} and also $\nu_{\text{O-H}}$ absorption peak of hydroxyl groups decreased in comparison with original WSF.

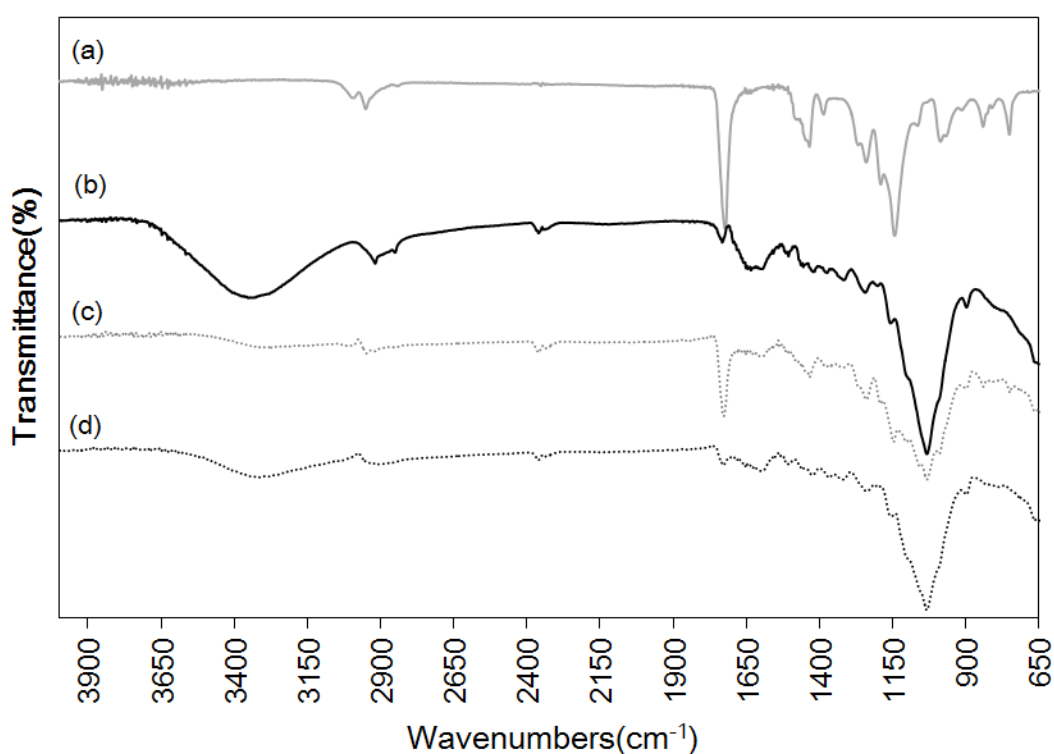


Figure 3-1. FT-IR spectra of PMMA (a), wheat straw fibers before (b) and after VASP of MMA (c), and extracted wheat straw fibers after VASP (d)

SEM images of the WSF before (Fig. 3-2a and b) and after VASP (Fig. 3-2c and d), and VWSF after extraction by Soxhlet method (Fig. 3-2e and f) were shown in Fig. 3-2. The surface morphology on WSF was significantly changed because of PMMA deposition after VASP of MMA. Though VWSF showed PMMA deposition, VWSF after washing with

CHCl_3 by Soxhlet method could not observe the polymer accumulation from SEM images even if we confirmed the PMMA on WSF surface after extraction in FTIR spectra.

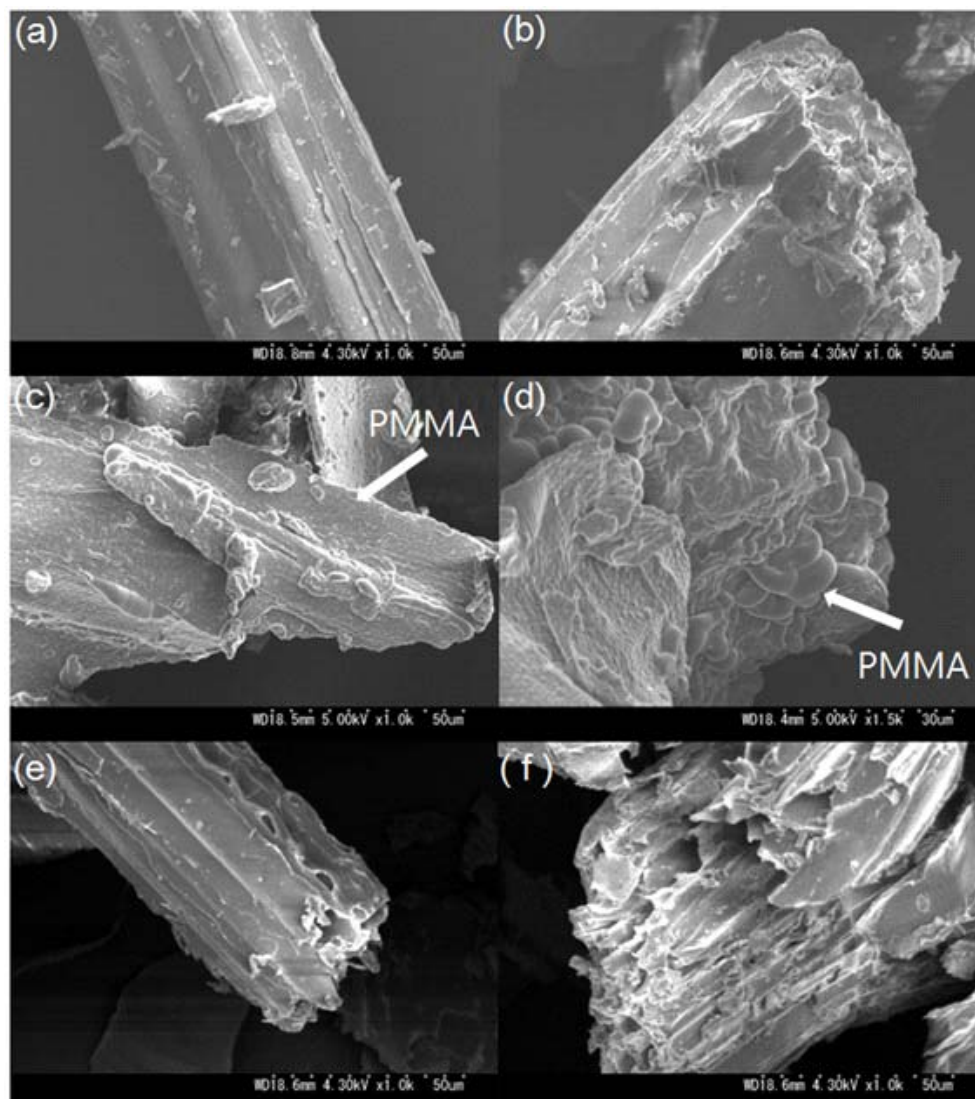


Figure 3-2. SEM images of wheat straw fibers before (a, b) and after VASP of MMA (c, d), and extracted wheat straw fibers after VASP (e, f)

In order to investigate thermal degradable behavior, WSF and VWSF were analyzed by TG and differential TG (DTG) as shown in Fig. 3-3. As can be seen from degradation curve

of WSF in Fig. 3-3, the WSF was decomposed around 200 °C, and its maximum rate of weight loss occurred at 310 °C. On the other hand, the TG/DTG profiles of VWSF showed two narrow weight loss regions of 240-340 °C and 340-410 °C corresponding to the degradation of WSF and PMMA components, respectively. This result suggested that the VWSF had slightly higher thermal stability than pristine WSF, and the thermal stability might be induced by specific interactions at interfaces between the WSF and the accumulated PMMA layers. After extraction of VWSF in CHCl₃ with Soxhlet apparatus, degradation behavior of VWSF after washing showed higher thermal stability than that of WSF. This result suggests that PMMA was grafted on WSF surface after VASP. Therefore, one of the causes in thermal stability increasing will be different heat conductivity of PMMA at surface of fine structured WSF [25].

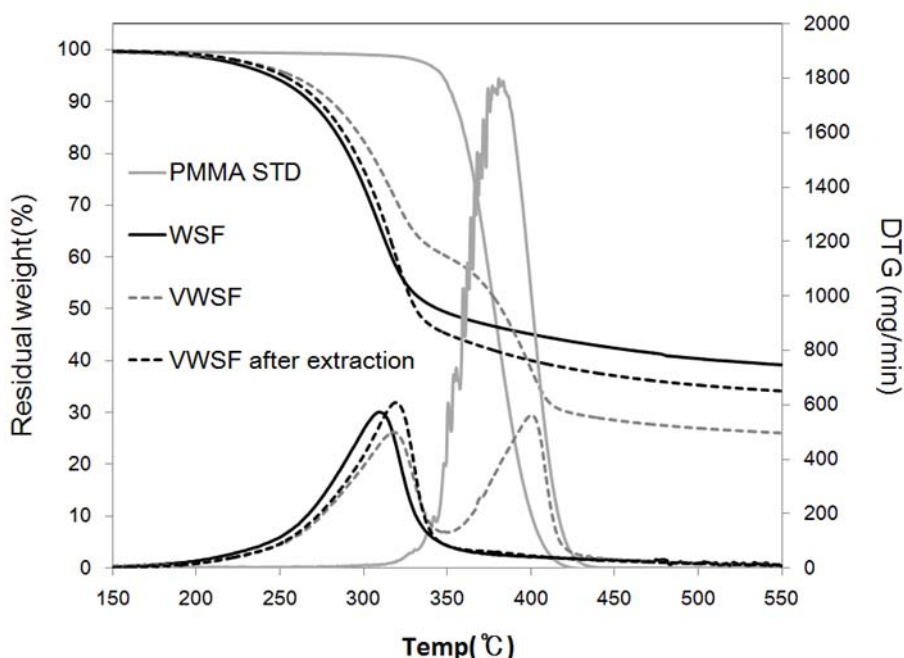


Figure 3-3. TG and DTG thermographs of commercial PMMA and wheat straw fibers before and after VASP of MMA, and washed wheat straw fibers after VASP

3.3.2 Characterization of PLLA/WSF and PLLA/VWSF composites

PLLA composite containing WSF and VWSF were prepared by twin screw extruder as listed in Table 3-2. To prepare the biocomposites using PLLA, the most WSF fibril width was between 63 and 106 μm after sieving. Two kinds of fiber and three proportion of fibers content of 5, 15, 30 wt% were used in the sample preparation. To determine the molecular weight of the extruded PLLA with fiber, a free polymeric component dissolved in CHCl_3 . The number- and weight-average molecular weights, analyzed by SEC, of the isolated polymer were listed in Table 3-2. A SEC result of original PLLA was $M_w = 14.7 \times 10^4$ and $M_w/M_n = 2.0$. The molecular weight distribution of extracted PMMA indicated very wide value affected to a feature of accumulation polymer after VASP process. The extruded PLLA shows lower molecular weight value than original PLLA because of thermal degradation. Therefore, the resulting products in this study should be considered on a thermal degradation of PLLA during the extruded process. The SEC results of PLLA composites containing WSF indicated that their molecular weights gradually decrease with increasing in WSF component.

Table 3-2. Composition and SEC results of the PLLA composites containing WSF and VWSF

Entry	Sample	PLLA content (wt.%)	Fibers content (wt.%)	M_w ($\times 10^4$)	M_n ($\times 10^4$)	M_w/M_n
1	PLLA	100	0	14.7	7.2	2.0
2	5WSF95PLLA	95	5	14.0	7.2	2.1
3	15WSF85PLLA	85	15	13.8	6.6	2.1
4	30WSF70PLLA	70	30	12.7	6.0	2.1
5	5VWSF95PLLA	95	5	15.0	6.1	2.5
6	15VWSF85PLLA	85	15	17.0	6.3	2.7
7	30VWSF70PLLA	70	30	19.0	6.7	2.8

Fig. 3-4 shows the TG and DTG curves of extruded PLLA, original WSF, and the PLLA composites containing 30 wt% WSF and VWSF. Though thermal degradation of PLLA showed a single degradation curve at 370 °C, the degradation temperature of PLLA composites was lower 60-70 °C than that of PLLA. On the other hand, degradation curve of WSF gradually decreased from 200 to 350 °C. This is because the acceleration of degradation might cause differences of heat conductivity to PLLA at the interface of WSF in composites. The char residue of PLLA composite with WSF at 550 °C is about 12.5 wt %, larger than that (10.8 wt%) of PLLA composite with VWSF. Interestingly, however, PLLA composite with VWSF has higher thermal stability due to its barrier effect of accumulated PMMA in comparison with PLLA/WSF composites in DTG results. To clarify the cause of thermal stability of PLLA composites including PMMA deposited on WSF, we examined and compared the SEC results of PLLA extracted from each composite as shown in Fig. 3-5. Thermal degradation of extruded PLLA for the composites was slightly induced and it was caused by increase of volume ratio of WSF to PLLA in Fig. 3-4a. On the other hand, SEC results of extracted PLLA from PLLA/VWSF indicated the suppression of thermal degradation (Fig. 3-4b). These obtained SEC results also verify the barrier effect of accumulated PMMA on WSF.

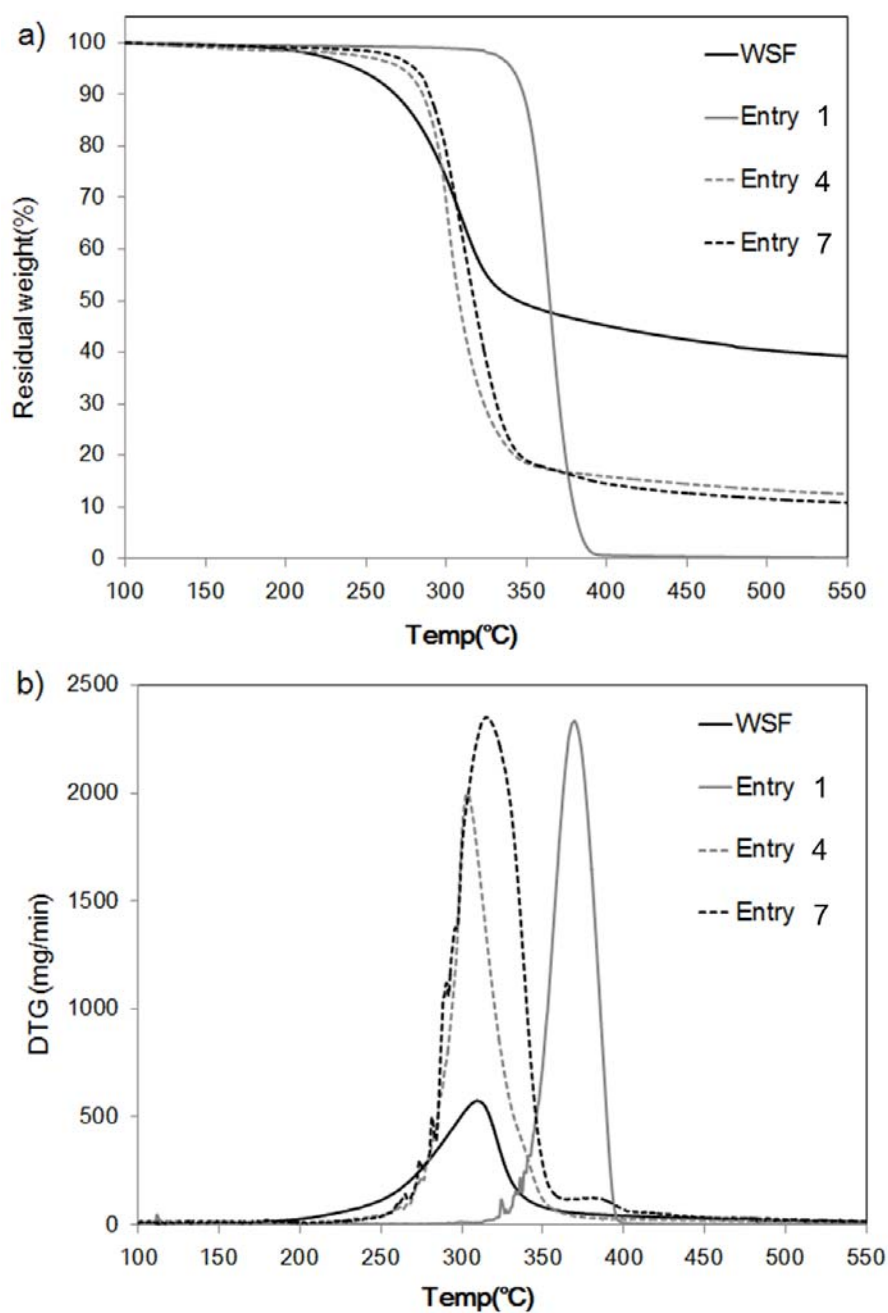


Figure 3-4. TG (a) and DTG (b) thermographs of neat PLLA and wheat straw fibers before and after VASP of MMA filled PLLA composites (Entry 1: PLLA, Entry 4: PLLA/WSF 30wt% and Entry 7: PLLA/VWSF 30wt% composites)

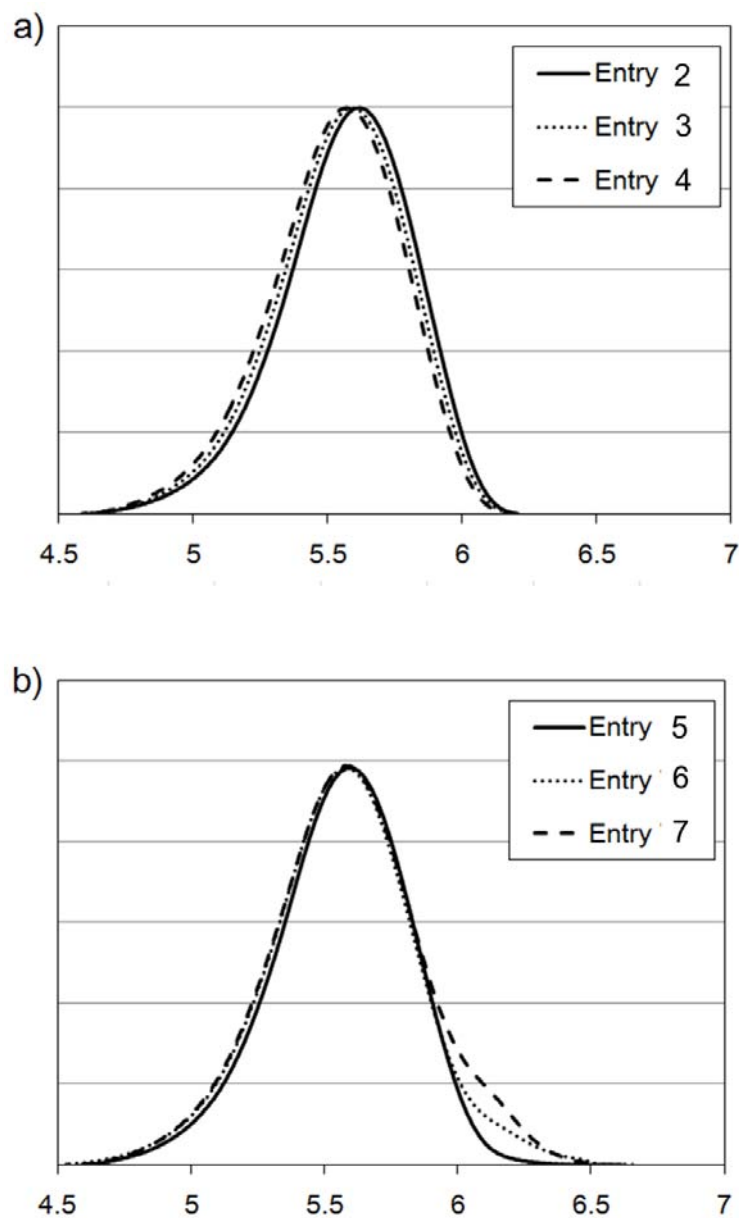


Figure 3-5. SEC profiles of PLLA/5, 15, 30 wt% WSF composites (a) and PLLA/5, 15, 30 wt% VWSF composites (b)

The tensile properties in the composites at the presence of cellulosic fibers can improve the mechanical properties of the composites causing several factors such as the nature of reinforcement fiber, fiber aspect ratio, fiber-matrix interfacial adhesion, and the fiber orientation in the composites [27]. One of the most important parameters controlling the

mechanical properties of short fibers composite is compatibility of fibers in the polymer matrix. Interfacial affinity between filler and polymer matrix is very important in fibers reinforced composites, as it indicates potential strength properties. In order to investigate the potential of WSF as reinforcement for PLLA and to determine whether it could be possible to improve the interfacial affinity between WSF and PLLA, mechanical properties of PLLA/WSF were evaluated and compared with that of PLLA/VWSF. Strength properties of PLLA/VWSF expected to be higher than the PLLA/WSF. Tensile testing data are shown in Fig. 3-6.

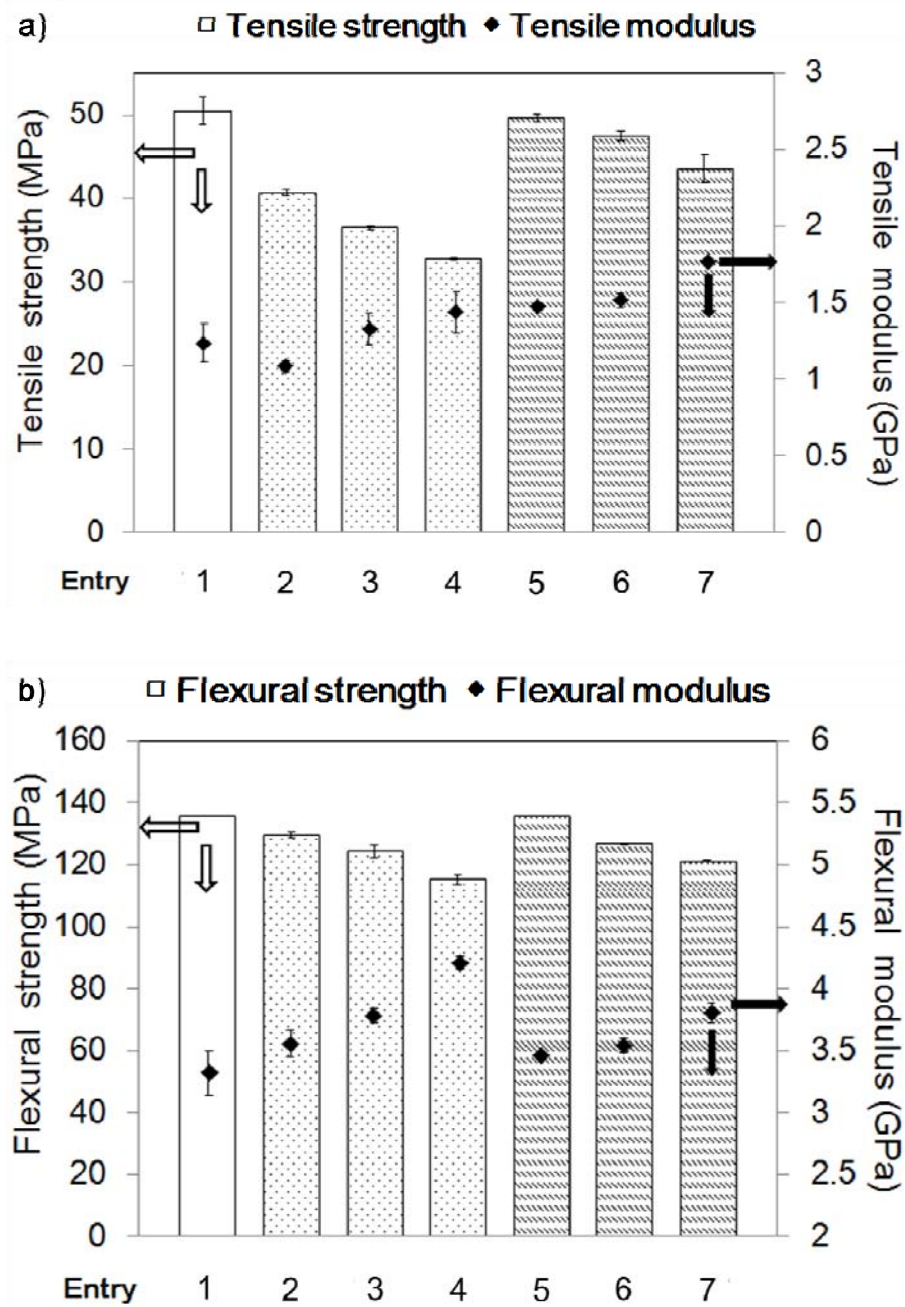


Figure 3-6. Tensile (a) and Flexural (b) data for PLLA with various amounts of WSF fibers

Nyambo *et al.* studied the preparation of green renewable composites based on PLA and 30 wt % of agricultural natural fibers such as corn stover, wheat straws, soy stalks, and hybrid fibers using twin screw extrusion followed by injection molding and evaluated interfacial adhesion of the fibers and matrix from the mechanical properties [28]. Commonly, it is observed that the value of tensile modulus or stiffness increases when fibers are used as

reinforcement in composites. The tensile strength of the composites showed a significant decrease resulting from the addition of 5, 15, and 30 wt% WSF to PLLA, while these were enhancing the tensile modulus. It is known that the modulus in natural agricultural fibers composites increase due to use as rigid filler that increases stiffness. The decrease of tensile strength in the composites could plausibly result from the incompatibility of the hydrophilic fibers and the hydrophobic polymer. However, the tensile strength was increased from 41 to 50 MPa in PLLA composite containing 5 wt% VWSF composites compared with PLLA/WSF, it indicated a similar value in the neat PLLA. Moreover, increase in tensile modulus was observed when the amount of VWSF is varied from 5 to 30 wt%. It's noteworthy that tensile strength of PLLA/VWSF composites was not only higher than that of PLLA/WSF composites but more enhancing the tensile modulus. These considerations strongly speak in favor of the concept that VASP process to cover the WSF surface with thin polymer layer can control the compatibility between the hydrophilic fibers and the hydrophobic polymer. Moreover, the composites with VWSF suppressed thermal degradation of PLLA which might be affected to the tensile strength.

The improvement of compatibility between fibers and polymer matrix can be seen under a scanning electron microscope (SEM) as shown in Fig. Fig. 3-7(a-d) obvious gaps are found between fibers and the PLLA matrix (Fig. 3-7a and b). Also, more fiber debonding is seen on the fracture surface of the PLLA/WSF samples. Through VASP process to WSF, VWSF fibers are well adhered to the PLLA matrix (Fig. 3-7c and d), and extensive fibers fracture with less fibers pull out is observed on the fracture surface. Saha et al. reported that the interfacial interaction affects the mechanical properties of the composite [29]. In order to demonstrate the higher tensile strength, it is important to modify the interphases adhesion between matrix polymer and fiber as filler. The results of mechanical tests indicate that

mechanical properties come under interfacial interaction influence. Herein, our VASP approach appeared to be well suited to control the compatibility between polymer matrix and filler for the construction of polymer composites.

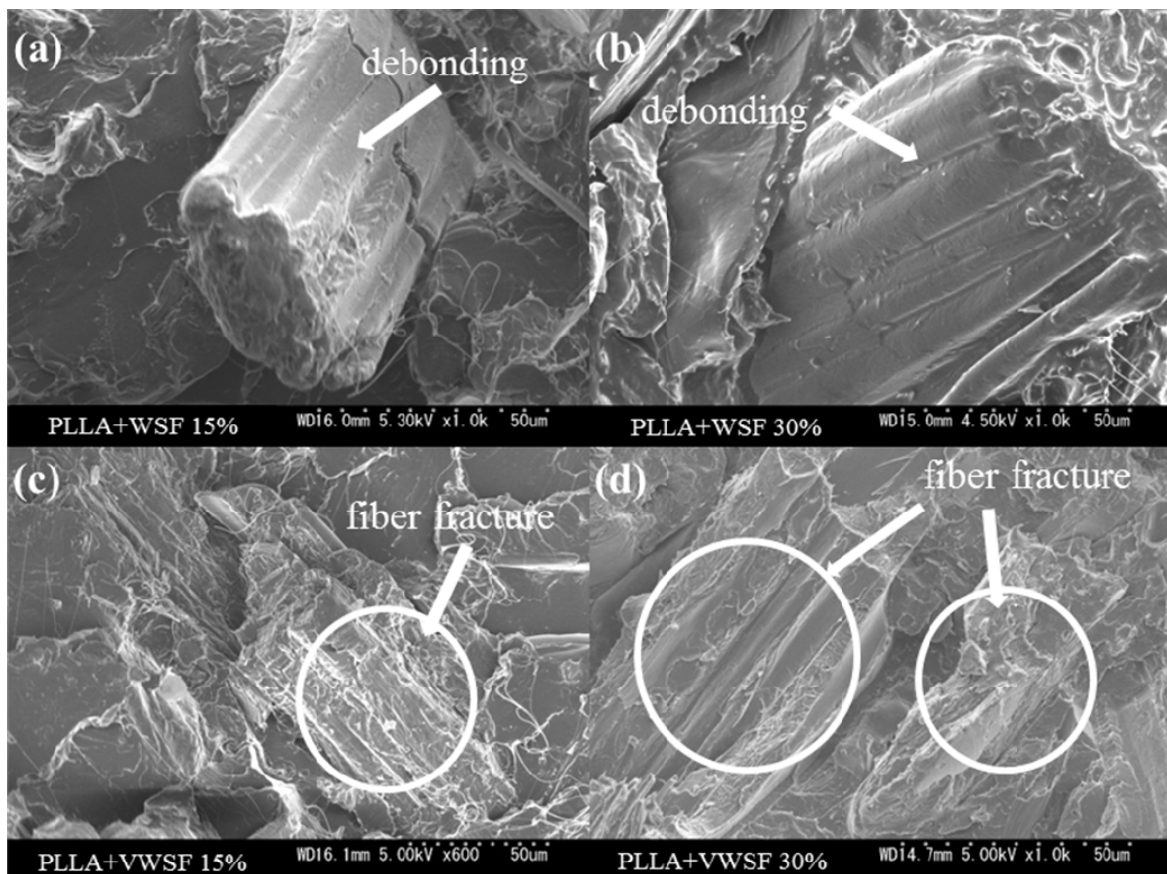


Figure 3-7. SEM images of PLLA / 15, 30 wt% WSF composites (a and b) and PLLA / 15, 30 wt% VWSF composites (c and d)

3.4 Conclusion

To conclude, the main purpose of this study was to construct the bio-based composite with wheat straw as waste agricultural residues. In order to achieve this purpose, we proposed VASP method as a novel pretreatment of fiber for improvement of compatibility in polymer matrix. PLLA composites containing 5, 15 and 30 wt% of each WSF with or without VASP of MMA were successfully prepared using twin screw extrusion followed by injection molding. Though the addition of the WSF to PLLA improved the tensile modulus and led to a decrease in the tensile strength, expression of its higher performance was achieved by application of pretreated WSF through VASP of MMA as a surface coating technique. Compared with unmodified WSF, the addition of VWSF in PLLA at various loadings from 5 to 30 wt% enhanced tensile modulus of resultant composites.

This study, through the use of VASP process for pretreatment of fibers, successfully showed good performance on tensile test. The compatibility between polymer matrix and fibers was discussed according to interphase morphologies and mechanical properties. Development of pretreatment system using VASP process for the good interphases adhesion between polymer matrix and fibers is an important development in the field of bio-based composites. The vapor-phase assisted surface polymerization (VASP) system can be greatly expected to improve the mechanical performance in polymer composite caused by improvement of compatibility between a polymer matrix and additives.

Acknowledgement

This work was supported by JSPS Grant-in-Aid for Scientific Research(A) 23241030.

3.5 References

- [1] Y. Andou, M. Yasutake, J-M. Jeong, H. Nishida, T. Endo. “Gas-Phase Assisted Surface Polymerization of Vinyl Monomers with Fe-Based Initiating Systems”, *Macromol Chem Physic.* (2005) 206, 1778-1783.
- [2] Y. Andou, M. Yasutake, J-M. Jeong, M. Kaneko, H. Nishida, T. Endo, “Gas-phase-assisted surface polymerization of methyl methacrylate with Fe(0)/TsCl initiator system”, *J Appl Polym Sci.* (2007) 103, 1879-1886.
- [3] D H. Kim, Y. Andou, Y. Shirai, H. Nishida, “Biomass-Based Composites from Poly (lactic acid) and Wood Flour by Vapor-Phase Assisted Surface Polymerization”, *Acs Appl Mater Inter.* (2010) 3, 385-391.
- [4] K.W. Kim, B.H. Lee, H.J. Kim, “Thermal and mechanical properties of cassava and pineapple flours-filled PLA bio-composites”, *J Therm Anal Calorim.* (2012) 108:1131–1139.
- [5] C. Nyambo, A. K. Mohanty, M. Misra, “Effect of Maleated Compatibilizer on Performance of PLA/Wheat Straw-Based Green Composites”, *Macromol. Mater. Eng.* (2011) 296, 710–718.
- [6] M. S. Huda, L. T. Drzal, M. Misra, A. K. Mohanty, K. Williams, D. F. Mielewski, “A Study on Biocomposites from Recycled Newspaper Fiber and Poly(lactic acid)”, *Ind. Eng. Chem. Res.* (2005) 44, 5593.
- [7] G. Grubbstrom, A. Holmgren, K. Oksman, “Silane-crosslinking of recycled low-density polyethylene/wood composites”, *Composites Part A.* (2010) 41, 678-683.
- [8] M. Bengtsson, K. Oksman, “Silane crosslinked wood plastic composites : Processing and properties”, *Compos. Sci. Technol.* (2006) 66, 2177-2186.
- [9] M. Bengtsson, K. Oksman, “The use of silane technology in crosslinking polyethylene / wood flour”, *Composites Part A.* (2006) 37, 752-765.
- [10] C S. Wu, “Renewable resource-based composites of recycled natural fibers and maleated polylactide bioplastic: Characterization and biodegradability”, *Polymer Degradation and Stability.* (2009) 94, 1076-1084.
- [11] H. Gao, Y M. Song, Q W. Wang, Z. Han, M L. Zhnag, “Rheological and mechanical properties of wood fiber-PP/PE blend composites”, *J. Fores. Rese.* (2008) 19, 315-318.
- [12] M. Yasutake, S. Hiki, Y. Andou, H. Nishida, T. Endo, “Physically controlled radical polymerization of vaporized vinyl monomers on surfaces. Synthesis of block copolymers of methyl methacrylate and styrene with a conventional free radical initiator”, *Macromolecules.* (2003) 36, 5974-5981.

- [13] Y. Matsumura, T. Minowa, H. Yamamoto, "Amount, availability, and potential use of rice straw (agricultural residue) biomass as an energy resource in Japan", *Biomass and Bioenergy*. (2005) 29, 347–354.
- [14] A. Alemdar, M. Sain, "Biocomposites from wheat straw nanofibers: Morphology, thermal and mechanical properties", *Compos. Sci. Technol.* (2008) 68, 557-565.
- [15] A. Alemdar, M. Sain, "Biodegradable nanocomposites from wheat straw", *In: Proceedings of the AIChE 2006 Annual Meeting. San Francisco, CA*, November 12–17, (2006).
- [16] N. Redddy, Y. Yang, "Preparation and Characterization of Long Natural Cellulose Fibers from Wheat Straw", *J. Agric. Food Chem.* (2007) 55, 8570–8575.
- [17] G.G.D. Silva, S. Guilbert, X. Rouau, "Successive centrifugal grinding and sieving of wheat straw", *Powder Technology*. (2011) 208, 266–270.
- [18] W.T. Mckean, R.S. Jacobs, "Wheat Straw as a Paper Fiber Source", *Clean Washington Center* (1997).
- [19] R.C. Sun, J.M. Fang, P. Rowlands, J. Bolton, "Physicochemical and Thermal Characterization of Wheat Straw Hemicelluloses and Cellulose", *J. Agric. Food Chem.* (1998) 46, 2804-2809.
- [20] X. Sun, R. Sun, Y. Su, J. Sun, "Comparative study of crude and purified cellulose from wheat straw", *J. Agric. Food Chem.* (2004) 52, 839–847.
- [21] M. Yasutake, S. Hiki, Y. Andou, H. Nishida, T. Endo, "Physically controlled radical polymerization of vaporized vinyl monomers on surfaces. Synthesis of block copolymers of methyl methacrylate and styrene with a conventional free radical initiator", *Macromolecules*. (2003) 36, 5974-5981.
- [22] Y. Andou, J -M. Jeong, S. Hiki, H Nishida, T. Endo, "Design of nanocomposites by vapor-phase assisted surface polymerization", *Macromolecules*. (2009) 42, 768-772.
- [23] Y. Andou, J -M. Jeong, S. Hiki, H Nishida, T. Endo, "Simple Procedure for Polystyrene-Based Nanocomposite Preparation by Vapor-Phase-Assisted Surface Polymerization", *Macromolecules*. (2009) 42, 7930-7935.
- [24] Y F. Buys, T. Aoyama, S. Akasaka, S. Asai, "Utilization of polymer degradation to modify electrical properties of poly(l-lactide)/poly(methyl methacrylate)/carbon filler composites", *Compos. Sci. Technol.* (2010) 70, 200-205.
- [25] A X. Jin, J L. Ren, F. Peng, F. Xu, G Y. Zhou, R C. Sun, J F. Kennedy, "Comparative characterization of degraded and non-degradative hemicelluloses from barley straw and maize stems: Composition, structure, and thermal properties", *Carbohydrate Polymers*. (2009) 78, 609-619.

- [26] R C. Sun, J. Tomkinson, "Characterization of hemicelluloses obtained by classical and ultrasonically assisted extractions from wheat straw", *Carbohydrate Polymers*. (2002) 50, 263-271.
- [27] J K. Sameni, S H. Ahmad, Z. Zakaria, "Effects of processing parameters and graft-copoly(propylene/maleic anhydride) on mechanical properties of thermoplastic natural rubber composites reinforced with wood fibers", *Plastics Rubber Composite*. (2012) 108, 1131-1139.
- [28] C. Nyambo, A K. Mohanty, M. Misra, "Polylactide-Based Renewable Green Composites from Agricultural Residues and Their Hybrids", *Biomacromolecule*. (2010) 11, 1654-1660.
- [29] A K. Saha, S. Das, D. Bhatta, B C. Mitra, "Study of jute fiber reinforced polyester composites by dynamic mechanical analysis", *J. Appl. Polym. Sci.* (1999) 71, 1505-1513.

Chapter 4. Design of surface coating on powdery fiber by gas-flow type of vapor-phase assisted surface polymerization (VASP-F)

4.1 Introduction

In previous Chapter 3, the coating method on natural fiber to control the interface adhesion between natural fiber and polymer matrix in agricultural waste (Wheat straw fibers)/polymer (PLLA) composite [1-3] had been discussed. VASP is an excellent method for preserving the fine structures of delicate substrate surfaces such as biomaterials in comparison with liquid and melt processes [4-11]. Moreover, VASP has additional advantage that the resulting product indicates some interactive effects at interface between the generated polymer and the substrate fiber. As results, polymer composite including wheat straw fiber as an agricultural waste after coating of PMMA through vapor-phase assisted surface polymerization (VASP) [12-15] shows higher performance in mechanical properties by tensile and flexural tests in comparison with untreated wheat straw fiber/polymer composite.

However, this methodology revealed bothersome problems to fabricate the agricultural waste/polymer composite in larger scale. In order to solve this scale-up problem on VASP method, some vulnerable points on the VASP process were paid attention for the effective polymerization; (1) Necessity of freezing the monomer under a high vacuum, (2) Polymerization progress under saturated vapor pressure of monomer, (3) Discontinuous feeding monomer in the system, and (4) Size limitation of VASP reactor. Therefore, the conventional VASP have been carried out under the limited conditions.

To overcome the bothersome points in the conventional VASP process, a gas-flow type of vapor-phase assisted surface polymerization (VASP-F) has been developed to ensure the surface coating on powdery natural fiber. VASP-F process could be polymerized on the substrate surface through monomer mist produced by monomer bubbling to cover on the surface. This report propose that VASP-F has many advantages for the control of polymerization reaction such as monomer feeding rate, non-limitation of reactor, and more simple reaction process.

In this Chapter 4, VASP-F was designed and optimized conditions for coating the fiber surface as similar as the resultant of conventional VASP. Instead of a conventional VASP, the procedure employs carrier gas including monomer mist under normal pressure such that the gaseous monomer is easily polymerized on the heated substrate. It has been our intention to demonstrate the simplified practicable VASP technique which employs easily handled for the natural fiber as a substrate.

4.2 Experimental

4.2.1 Materials

Monomer: MMA (Wako Pure Chemical Industries, Ltd.) was distilled under reduced pressure from CaH_2 just before polymerization. Substrate: wheat straw fibers (WSF) was purchased from National Agriculture and Food Research Organization (NARO) in Japan and used as received. Initiator: 2,2'-azobis(2,4-dimethylvaleronitrile)(ADMVN) and polymethyl

methacrylate (PMMA, M_w 100000) were purchased from Wako Pure Chemical Industries, Ltd. and used as received.

4.2.2 Grinding process

Wheat straw (4-5cm) was pulverized in twice by the pin mills (Pulverizer M-2 MILL Model Machine; NARA MACHINERY Co., Ltd, JAPAN) under 8000 rpm with a screen size (0.5 mm). The particles were sieved by sieving machine (AS-200 model machine; Retsch Co., Ltd, JAPAN) to choose fiber size 150-250 μm . The wheat straw fibers (WSF) were dried in an oven at 80 $^{\circ}\text{C}$ for 48 h, and stored in polyethylene bags until use.

4.2.3 General procedure of VASP-F of MMA

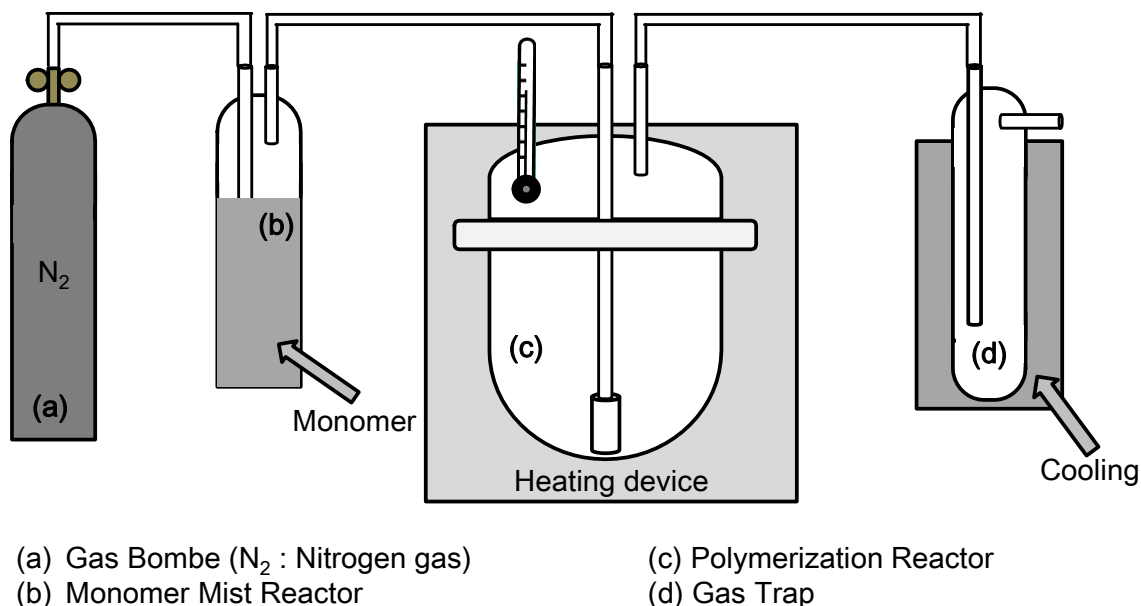


Figure 4-1. Schematic illustration of the VASP-F reaction system

Before VASP, to adsorb the initiator ADMVN on the WSF surface, WSF (ca.50g) was treated with a 99.5% acetone solution (200 mL) of ADMVN at a 1/20 weight ratio to WSF at 25 °C for 1 h under stirring. After the treatment, acetone was removed at room temperature, resulting in the production of powdery WSF.

The VASP-F reactor designed to grow vinyl polymer by the above scheme is shown schematically in Fig. 4-1. The reaction vessel is a cylindrical Schlenk flask tube 125mL of diameter 3.5 cm and length 13 cm (VIDREX CO., LTD, JAPAN) and Flask reaction 1000mL (AS ONE CO., LTD, JAPAN) of diameter 12.5 cm and length 13 cm. The initiator-adsorbed WSF (ca. 2, 7.5, 30 and 75 g) was put into the bottom of glass reactor. A regulated stream of pure N₂ gas is introduced into the heating glass vessel to provide a slight pressure gradient, causing the vinyl monomer vapor to flow along the reactor tube. The glass vessel is heated using oil bus.

MMA as a vinyl monomer is loaded into a 125 ml size of bubbler, the temperature of which is maintained by a silicone oil bath. Pure nitrogen gas, regulated to 200ml/min, passes through a flow meter and bubbles through the MMA, thereby carrying MMA vapor through a silicone transfer tube into the reaction vessel. The MMA reacts to form PMMA on substrates, excess unreacted MMA vapor, and any volatile side-reaction products, are exhausted and trapped in the cold glass-trap.

After VASP-F of MMA, obtained product was dried to remove adsorbed unreactant in vacuo and weighed to yield the PMMA/WFS composite (VWSF). The product was analyzed intact with Fourier transform infrared (FTIR) spectroscopy, scanning electron microscopy (SEM), and thermogravimetry (TG). Free-polymers on VWSF particle were extracted using CHCl₃ with a Soxhlet apparatus for 24 h. The isolated polymers were dried and analyzed by FTIR, thermogravimetry (TG) and size-exclusion chromatography (SEC).

4.2.4 Characterization

Fourier transform infrared (FTIR) spectra of WSF were recorded on a Perkin Elmer Spectrometer GX2000R. Reflection spectra were measured on a Golden Gate Diamond ATR (10500) module with a germanium crystal by the single-reflection ATR method. Molecular weights of the sample were measured by size exclusion chromatography (SEC) on a TOSOH HLC-8320 SEC system with a refractive index (RI: UV, $\lambda = 254$ nm) detector at 40 °C using a TOSOH TSKgel Super HM-M column (linearity range, 1×10^{-3} to 8×10^{-6} molecular weight exclusion limit, 4×10^{-8}) and chloroform (CHCl_3 : HPLC grade) eluent (0.6 mL min^{-1}). The calibration curves for SEC analysis were obtained using polystyrene standards with a low polydispersity (5.0×10^2 , $1.0^5 \times 10^3$, 2.5×10^3 , 5.87×10^3 , 9.49×10^3 , 1.71×10^4 , 3.72×10^4 , 9.89×10^4 , 1.89×10^5 , 3.97×10^5 , 7.07×10^5 , 1.11×10^6 , TOSOH Corporation). The sample (10 mg) was dissolved in chloroform (2 mL) and the solution was filtered through a membrane filter with a 0.45 μm pore size.

Thermal degradation behavior of VASP-F samples was analyzed by a thermogravimetry (TG). TG was conducted on a Seiko Instrumental Inc. EXSTAR 6200 TG/DTA system in an aluminum pan (5 mm ϕ) under a constant nitrogen flow (100 mL min^{-1}) using about 6-8 mg of film sample. Dynamic thermal degradation of the sample was conducted at prescribed heating rates, ϕ , of $10 \text{ }^\circ\text{C min}^{-1}$ in a temperature range of 40 to 550 °C.

WSF samples before and after VASP-F of MMA sputtered carbon by a HITACHI E-1030 instrument and they were observed by a HITACHI- S3000N scanning electron microscope (SEM) at an accelerating voltage of 4.0kV

4.3 Results and discussion

4.3.1. VASP-F of MMA on wheat straw fibers

Although a conventional VASP of MMA in H-shape reactor was carried out with azobisisobutyronitrile (AIBN) in previous chapter, VASP-F of MMA was not conducted with AIBN on the natural fiber. Since some particle shape of PMMA oligomer was found in exhaust silicone tube, it was supposed that AIBN might be detached and exhausted through monomer mist from fiber surface. Therefore, AIBN was changed to higher molecular weight of initiator; 2, 2'-azobis(2,4-dimethylvaleronitrile) (ADMVN) due to hardly exfoliate from the substrate [16-18]. It was confirmed that the resulting VASP-F of MMA was proceeded as listed in Table 4-1.

Table 4-1. Results of VASP-F of MMA on surface of wheat straw fibers (WSF)

Entry	WSF (g)	VASP-F (8h)			Increment (wt%)	M_w ($\times 10^3$)	M_w/M_n	Recovery monomer (%)
		Temp. (°C)	N ₂ flow ratio (mL/min)	Supply volume rate of MMA (mL/h)				
1	7.52	80	200	2.6 \pm 0.1	3.1	1.9	1.9	93 \pm 1
2	7.55	80	400	6.1 \pm 0.1	1.8	1.4	1.3	95 \pm 2
3	7.51	100	200	2.6 \pm 0.1	3.7	2.6	1.9	90 \pm 1
4	7.59	110	200	2.6 \pm 0.1	2.3	1.6	1.5	94 \pm 1
5	7.48	120	200	2.6 \pm 0.1	1.6	1.4	1.3	95 \pm 1

To investigate polymerization condition, VASP-F of MMA was conducted under various conditions such as reaction temperature and gas flow rate. To determine the molecular weight of the resulting product on WSF, a free polymeric component was dissolved with CHCl₃. The number- and weight-average molecular weights, analyzed by SEC. VASP-F of MMA at 80 °C for 8 h under 200ml/min of N₂ gas flow rate showed higher increment than

the case of 400ml/min(Entry 1 and 2). This result shows that ADMVN might be also exfoliate from the substrate surface to outside of the system under high gas flow rate. The reactions temperature on which VASP-F of MMA yield more efficiently were examined, and the optimal condition was established. VASP-F of MMA was carried out at 100⁰C for 8 h under 200ml/min, the resulting products showed the highest increment and molecular weight compared to other reaction temperature. Since ADMVN half-life of temperature is 51⁰C, the degradation of initiator in the resulting was induced under higher polymerization temperature (Entry 1, and 3-5).

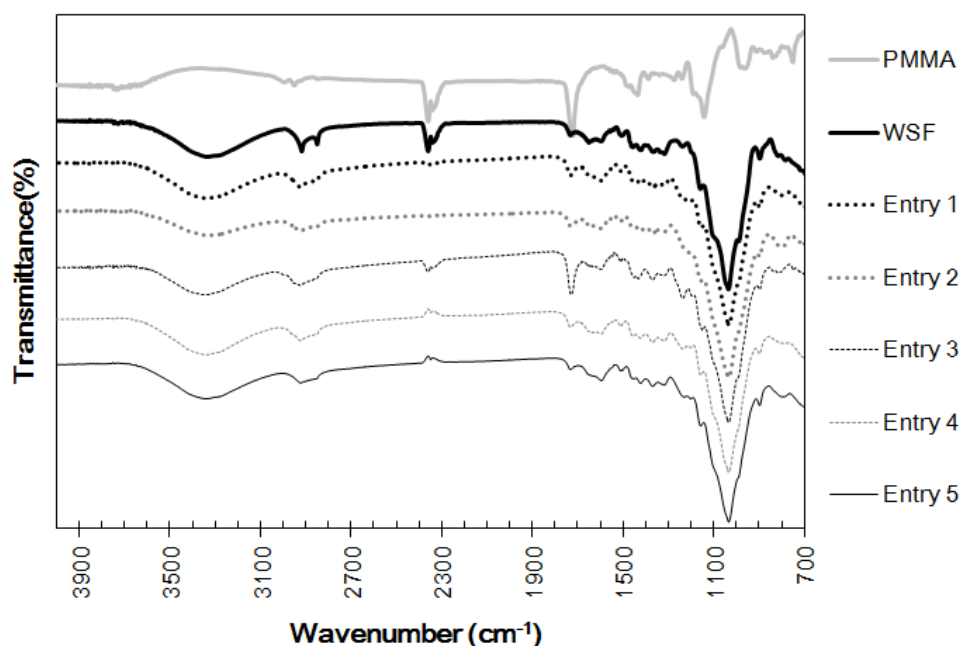


Figure 4-2. FT-IR spectra of PMMA (a), wheat straw fibers before (b) and after VASP-F of MMA (Entry 1-5)

Fig. 4-2 shows significant changes from FTIR spectra of polymer deposited on WSF comparing with commercially available PMMA and untreated WSF upon VASP-F of MMA. The FTIR spectra of WSF after VASP-F of MMA and a commercial available PMMA

exhibited the same characteristic peaks at 1721 cm^{-1} assignable to $\nu_{\text{C=O}}$ [19-22]. Interestingly, WSFs after VASP-F of MMA still shows a broad peak in the wavenumber range of $3100\text{--}3700\text{ cm}^{-1}$ attribution to $\nu_{\text{O-H}}$ of hydroxyl groups in WSF even though VWSF showed 1721 cm^{-1} attribution to $\nu_{\text{C=O}}$. These results indicate that the surfaces were insufficiently covered by accumulated materials. Therefore, the condition on VASP-F of MMA should further optimize to obtain WSF sufficiently covered with PMMA. VASP of MMA at $100\text{ }^{\circ}\text{C}$ under 200 mL/min of N_2 gas flow on WSF was conducted with varied reaction time as listed in Table 4-2.

Table 4-2. Results of VASP-F of MMA with varied reaction time

Entry	WSF (g)	ADMVN ^(a) (mg/g)	Time (h)	Supply volume rate of MMA (mL/h)	Weight Increment (wt%)	M_w ($\times 10^3$)	M_w/M_n	Recovery monomer (%)
1-1	2.02	50	6	2.4 ± 0.1	2.4	1.7	2.8	90 ± 1
1-2	2.03	50	12	2.5 ± 0.1	3.1	2.9	3.9	89 ± 2
1-3	2.07	50	18	2.5 ± 0.1	3.7	3.8	4.5	88 ± 1
1-4	2.08	50	24	2.5 ± 0.1	4.2	4.6	4.9	87 ± 1

(a) ADMVN : 2,2'-azobis(2, 4-dimethyl)valeronitrile

The polymerization with ADMVN proceeded smoothly on the WSF surface at $100\text{ }^{\circ}\text{C}$ (sample 1-4). The homopolymer PMMA obtained through the VASP-F was completely soluble in conventional solvents for corresponding polymers prepared by a Soxhlet process. In SEC analysis, the polymer obtained high molecular weight ($1.7 \times 10^3\text{--}4.6 \times 10^7\text{ Da}$ in M_w). Table 4-2 shows the changes in polymer yield on the VASP-F of MMA with different reaction time. The SEC results shifted to higher molecular weights with time and then gradually changing of M_w/M_n values into a bimodal or multimodal profile. Each plot of M_w

and M_n vs PMMA yield per initiator concentration on the substrate surface converged to one line (Fig. 4-3). These results suggest that the growing chain ends continued to propagate with a long lifetime, and after an initial period the subsequent initiation process was reduced. As a result of WSF after VASP-F of MMA, this implies a hydrophilic surface property of the fibers has been replaced by hydrophobic by effect of fiber coating on the surface of the PMMA (Fig. 4-4).

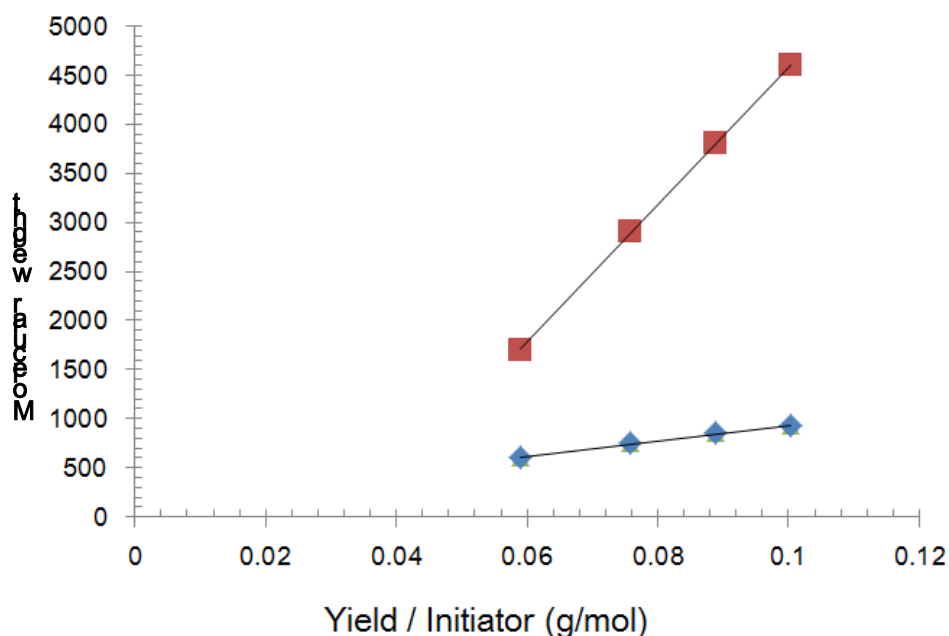


Figure 4-3. Relationship between the molecular weight and yield per initiator

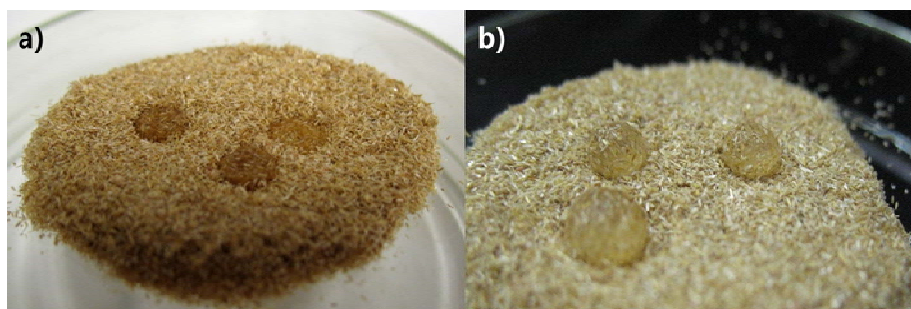


Figure 4-4. Results of surface property of WSF before and after (Entry 1-4) VASP-F of MMA to water droplets

Considering the 10 h half-life temperature of ADMVN is 55 °C, a considerable amount of ADMVN must have accelerated to generate radical species during the VASP-F at 100 °C. Though the VASP-F should appear in the lower molecular weight region, SEC profiles do not show newly occurring polymer chains because of increasing of molecular weights and PDI values. The time-course test results of the VASP-F of MMA indicated that the growing chain ends had a long lifetime on the surfaces.

The WSF after VASP-F of MMA (VWSF) was investigated by TG-DTA to reveal their thermal degradation properties comparing with that of WSF as shown in Fig. 4-5. Thermal degradation behaviors of WSF indicated four degradation steps from its TGA curve. First step is removing moisture from fiber around 100 °C, and then hemicellulose component degraded in 150 °C -250 °C. Furthermore, cellulose component was degraded from 250 °C to 330 °C, and lignin component was degraded above 330 °C as a last step. [23, 24]

DTG results indicated that degradation temperature of VWSF was slightly increased comparing with WSF [25]. Degradation behavior of PMMA showed around 320-430°C in DTG profile. This result suggested that the VWSF had slightly higher thermal stability than pristine WSF, and this higher thermal stability might be affected by specific interactions at interfaces between the WSF and the accumulated PMMA layers. The deposition of PMMA on WSF revealed to exist in DTG profile of Entry 1-4. Moreover, peaks in DTG profiles corresponding to WSF component in VWSF slightly shifted to higher temperature side in comparison with pristine WSF. PMMA component on VWSF was washed by Soxhlet method with CHCl₃. The washed WSF also indicated higher degradation temperature than WSF before VASP-F. From the DTG profiles, it is supposed that PMMA was grafted on WSF fiber using VASP-F of MMA.

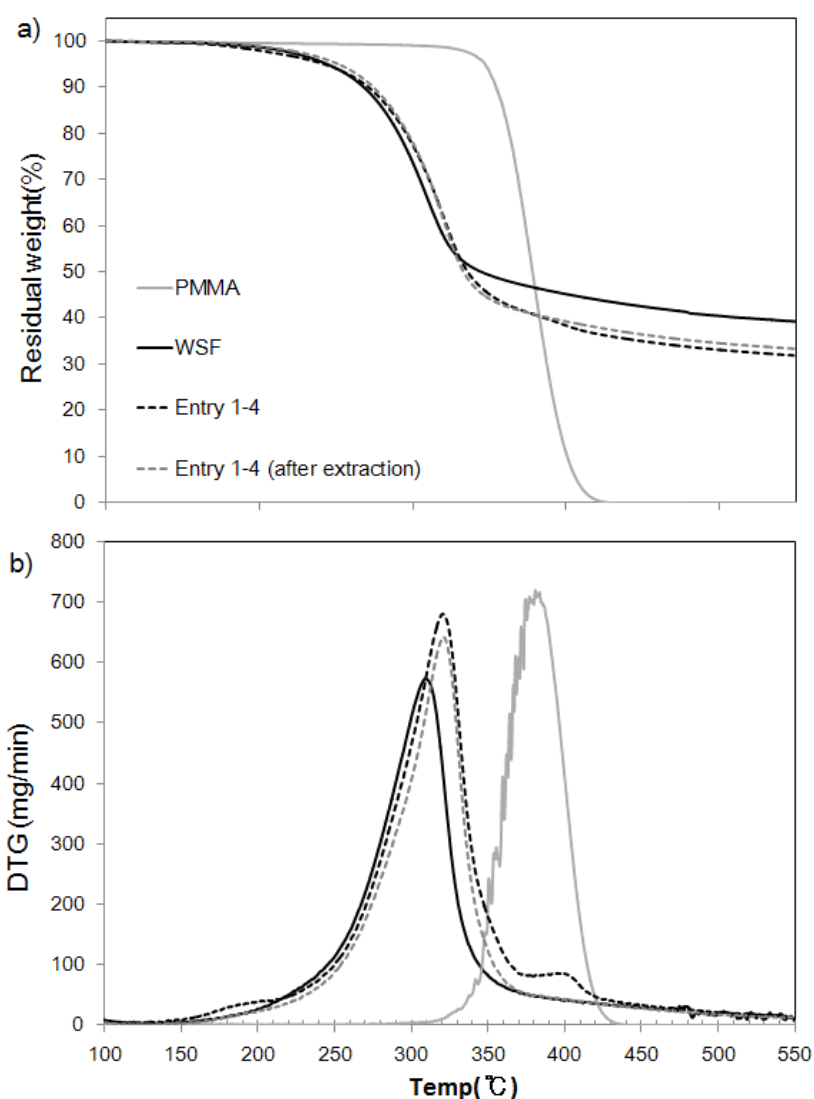


Figure 4-5. TG and DTG thermographs of commercial PMMA and WSF before and after VASP-F of MMA

To confirm the newly accumulated materials on the WSF surfaces after VASP-F of MMA, the product, Entry 1-4 in Table 4-3, was extracted using CHCl_3 with a Soxhlet extraction apparatus. These samples were measured by FTIR spectra as shown in Fig. 4-6. FTIR spectra of the samples and a commercial available PMMA exhibited the same characteristic peaks as 1721 cm^{-1} corresponding to $\nu_{\text{C=O}}$ in PMMA. The peak at 1730 cm^{-1} for carbonyl stretching in WSF is attributed to hemicellulose [26, 27]. Interestingly, when the accumulated PMMA layers were removed using CHCl_3 with a Soxhlet extraction apparatus,

the residual WSF ingredient showed nearly the same FT-IR spectrum as the original WSF. However, the $\nu_{\text{C=O}}$ absorption peak on residual VWSF surfaces after the extraction treatment also appeared at 1721 cm^{-1} and also $\nu_{\text{O-H}}$ absorption peak of hydroxyl groups decreased in comparison with original WSF. This result also indicated that PMMA was grafted on the WSF surface by VASP-F of MMA.

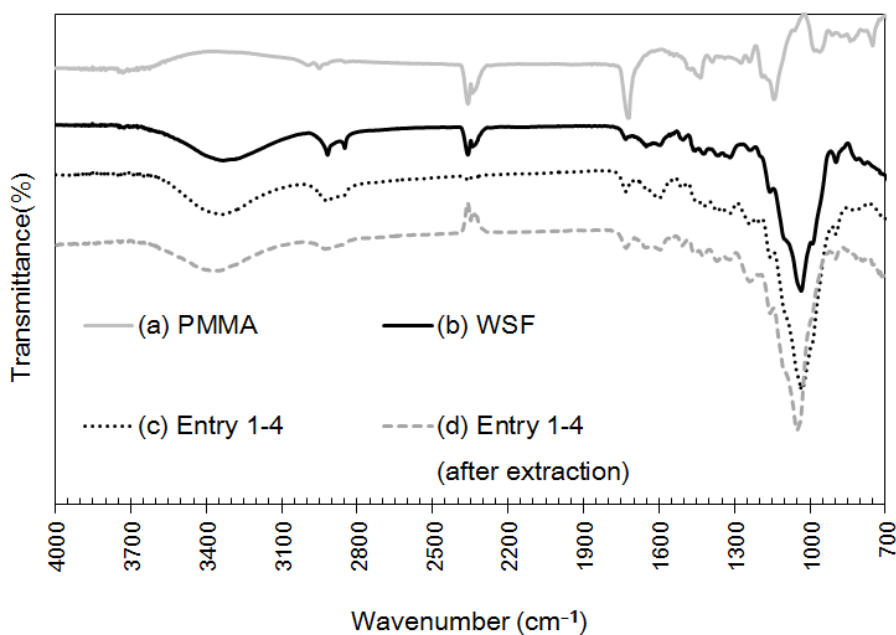


Figure 4-6. FT-IR spectra of PMMA (a), wheat straw fibers before (b) and after VASP-F of MMA(c), and WSF after extraction with CHCl_3 (d)

It was found that construction of VASP-F was desirable results for modification of substrate surface. To give large amounts of surface modified substrate, reactor size was scaled up from 125mL to 1000mL for VASP-F. The VASP-F of MMA on WSF with scale-up reactors was conducted to gain optimum condition for improvement of surface property as listed in Table 4-3.

Table 4-3. Results of VASP-F of MMA on WSF in scale-up reactor^{a)}

Entry	WSF ^{b)} (g)	VASP-F			Weight Increment (%)	M_w ($\times 10^3$)	M_w/M_n	Monomer recover (%)
		N ₂ flow ratio (mL/min)	Supply volume rate of MMA (mL/h)	Monomer bottle (°C)				
3	7.51	200	2.6 \pm 0.1	25	3.7	2.6	1.9	90 \pm 1
6	7.52	200	19.5 \pm 0.9	50	8.0	7.1	4.8	85 \pm 2
7	30.25	200	19.5 \pm 1.0	50	4.3	2.9	2.0	92 \pm 2
8	30.44	400	45.2 \pm 2.1	50	8.1	7.3	4.9	85 \pm 2
9	75.12	400	45.0 \pm 1.9	50	5.8	3.7	3.5	88 \pm 2

^{a)} Reaction conditions: VASP-F was carried out with MMA on WSF for 8h at 100 °C.

^{b)} Initiator deposition ratio: $0.05 \text{ g}^{\text{ADMVD}}/\text{g}^{\text{WSF}}$

Firstly, VASP-F of MMA with WSF in 1000ml flask as a reactor was carried out under maintaining optimum condition (Entry 3). However, increment of PMMA on WSF after VASP-F in large reactor was lower than the case of small reactor under same condition. In the large reactor, monomer concentration became low in comparison with the small reactor because supply monomer volume was constant (Entry 3 and 6). In order to increase the polymer increment and M_w values, supply volume of monomer was increased from a monomer mist reactor by heat such as a heating oven and an oil bus. Therefore, VASP-F of MMA was more smoothly proceed through monomer with heat. However, this method was insufficient to get enough yields for larger quantity of substrate (Entry 7). To optimize a VASP-F method for large amounts of substrates, it was considered that control of gas-flow rate was a countermeasure against large quantity of substrate (Entry 8). As a result, VASP-F of MMA with large amounts of WSF was sufficiently preceded by controlling the monomer temperature and gas-flow rate in the system (Entry 9).

FT-IR analysis revealed the compositional changes on WSF fiber before and after VASP-F of MMA as shown in Fig. 4-7. The presence of carboxyl group attribution to PMMA shows at $1,721 \text{ cm}^{-1}$ in FTIR spectra (Entries 6-9). As for each WSF samples

provided with large reactor, it was confirmed that WSF was covered with PMMA through VASP-F of MMA by FTIR analysis, respectively. As a result, VASP-F system for the modification of substrate surface provides a method, which can be easily scaled up, at low costs and in a high yield.

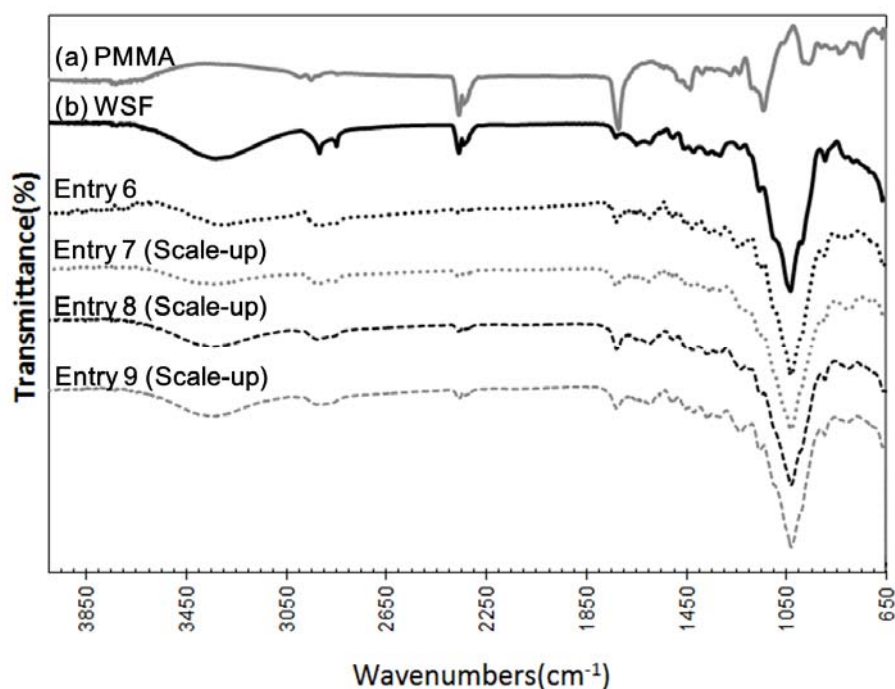


Figure 4-7. FT-IR spectra of WSF (a), wheat straw fibers before (b) and after VASP-F of MMA(Entry 6-9)

In order to investigate changes in the morphology of the fibers in terms of size and level of smoothness, Fig. 4-8 shows SEM images of WSF before and after VASP-F of MMA. The SEM images provide evidence on changes in the fiber morphology as a result of the VASP-F employed. Fig. 4-8 (a) and (b) shows the morphology of the untreated WSF (raw material) while the morphology of the accumulated polymer like laminate surface of fibers is displayed in Fig. 4-8(c) and (d). Therefore, it was revealed that the PMMA was deposited on WSF surface after VASP-F of MMA.

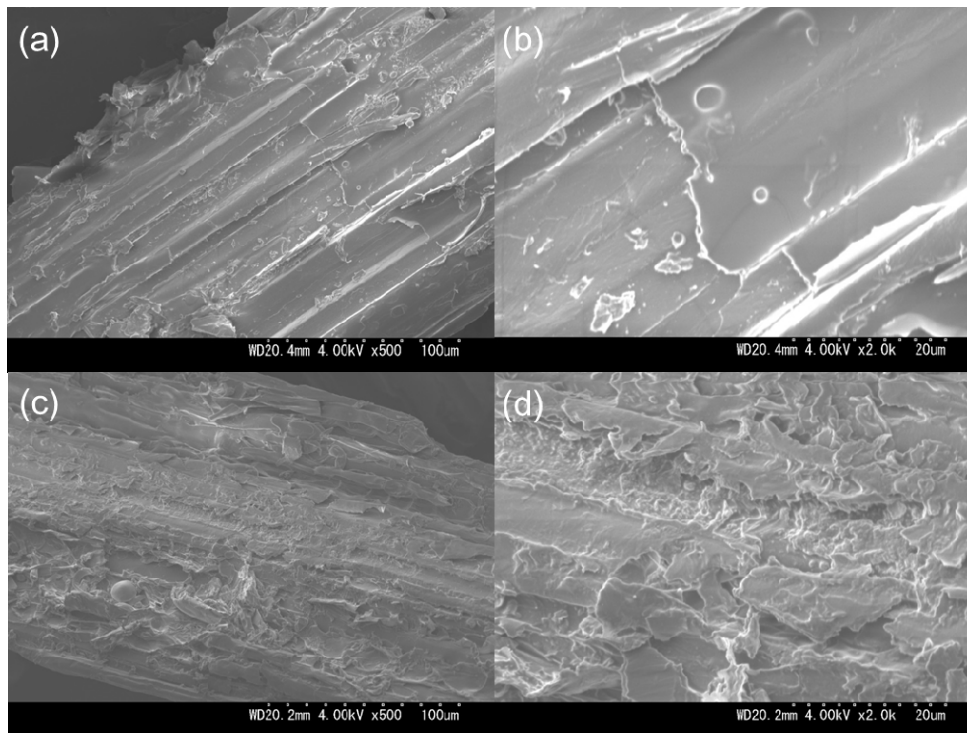


Figure 4-8. SEM micrographs of wheat straw fibers before (a-b) and after VASP-F of MMA, Entry 8 (c, d)

4.4 Conclusion

In conclusion, the main purpose of this chapter 4 was to the proposed VASP-F method as a novel pretreatment of fiber for improvement of compatibility in polymer matrix. In order to demonstrate the higher mechanical strength in polymer composite, it is important to modify the interphases adhesion between matrix polymer and fiber as filler. In order to obtain larger volume of surface modified powdery substrates, I succeeded in constructing the gas-flow type of vapor-phase assisted surface polymerization (VASP-F) using provision of nitrogen gas containing monomer mist. The deposition rate of polymer on a substrate surface in VASP-F had been controlled using optimal gas flow-rate and monomer and reactor temperature. This polymerization system can inherit advantages of VASP method due to

polymer grafted on substrate and to collect waste or reactant monomer as a recycle. That is, the VASP-F is not only the physically controlled process as same as VASP but it can be simpler scale-up for practical use.

4.5 References

- [1] R. Pradhan, M. Misra, L. Erickson, A. Mohanty, “Compostability and biodegradation study of PLA–wheat straw and PLA–soy straw based green composites in simulated composting bioreactor”, *Bioresource Technology*. (2010) 101, 8489-8491.
- [2] C. Nyambo, A. K. Mohanty, M. Misra, “Effect of Maleated Compatibilizer on Performance of PLA/Wheat Straw-Based Green Composites”, *Macromol. Mater. Eng.* (2011) 296, 710-718.
- [3] C. Nyambo, A. K. Mohanty, M. Misra, “Polylactide-Based Renewable Green Composites from Agricultural Residues and Their Hybrids”, *Biomacromolecules*. (2010) 11, 1654-1660.
- [4] M. Yasutake, Y. Andou, S. Hiki, H. Nishida, T. Endo, “Controlled Radical Polymerization of Vaporized Vinyl Monomers on Solid Surfaces under UV Irradiation”, *Macromol Chem Physic.* (2004) 205, 492-499.
- [5] M. Yasutake, Y. Andou, S. Hiki, H. Nishida, T. Endo, “Physically controlled, free-radical polymerization of vaporized fluoromonomer on solid surfaces”, *Journal of Polymer Science Part A: Polymer Chemistry*. (2004) 42, 2621-2630.
- [6] Y. Andou, M. Yasutake, J-M. Jeong, H. Nishida, T. Endo. “Gas-Phase Assisted Surface Polymerization of Vinyl Monomers with Fe-Based Initiating Systems”, *Macromol Chem Physic.* (2005) 206, 1778-1783.
- [7] Y. Andou, H. Nishida, T. Endo, “Designed surface construction by photo-induced vapor-phase assisted surface polymerization of vinyl monomers using immobilized free radical initiators”, *Chemical Communications*. (2006) Issue 48.
- [8] Y. Andou, M. Yasutake, H. Nishida, T. Endo, “Designed Surface Modification by Photo-induced Vapor Phase Assisted Surface Polymerization of Vinyl Monomers”, *Journal of Photopolymer Science and Technology*. (2007) 20, 523-528.
- [9] Y. Andou, M. Yasutake, J-M. Jeong, M. Kaneko, H. Nishida, T. Endo, “Gas-phase-assisted

- surface polymerization of methyl methacrylate with Fe(0)/TsCl initiator system”, *J Appl Polym Sci.* (2007) 103, 1879-1886.
- [10] Y. Andou, J-M. Jeong, S. Hiki, H. Nishida, T. Endo, “Design of Nanocomposites by Vapor-Phase Assisted Surface Polymerization”, *Macromolecules.* (2009) 42, 768-772.
- [11] Y. Andou, J-M. Jeong, H. Nishida, T. Endo, “Simple Procedure for Polystyrene-Based Nanocomposite Preparation by Vapor-Phase-Assisted Surface Polymerization”, *Macromolecules.* (2009) 42, 7930-7935.
- [12] M. Yasutake, S. Hiki, Y. Andou, H. Nishida, T. Endo, “Physically Controlled Radical Polymerization of Vaporized Vinyl Monomers on Surfaces. Synthesis of Block Copolymers of Methyl Methacrylate and Styrene with a Conventional Free Radical Initiator”, *Macromolecules.* (2003) 36, 5974-5981.
- [13] H. Nishida, M. Yamashita, Y. Andou, J-M. Jeong, T. Endo, “Gas-Phase Assisted Surface Polymerization Behavior of ϵ -Propiolactone on Inorganic and Organic Substrates and Consequent Composite Production”, *Macromol Mater Eng.* (2005) 290, 848-856.
- [14] Y. Andou, J-M. Jeong, M. Kaneko, H. Nishida, T. Endo, “Hydrophobic cellulose fiber surfaces modified with 2,2,3,3,3-pentafluoropropylmethacrylate (FMA) by vapor-phase-assisted photopolymerization”, *Polym J.* (2010) 42, 519-524.
- [15] D H. Kim, Y. Andou, Y. Shirai, H. Nishida, “Biomass-Based Composites from Poly (lactic acid) and Wood Flour by Vapor-Phase Assisted Surface Polymerization”, *Acs Appl Mater Inter.* (2010) 3, 385-391.
- [16] C. M. Tseng, Y. Y. Lu, M. S. El-aasser, J. W. Vanderhoff, “Uniform Polymer Particles by Dispersion Polymerization in Alcohol”, *Journal of Polymer Science: Part A.* (1986) 24, 2995-3007.
- [17] K. A. Shaffer, T. A. Jones, D. A. Canelas, J. M. DeSimone, “Dispersion Polymerizations in Carbon Dioxide Using Siloxane-Based Stabilizers”, *Macromolecules.* (1996) 29, 2704-2706.
- [18] S. Shen, E. D. Sudol, M. S. El-Aasser, “Control of particle size in dispersion polymerization of methyl methacrylate”, *Journal of Polymer Science Part A: Polymer Chemistry.* (1993) 31, 1393-1402.
- [19] A X. Jin, J L. Ren, F. Peng, F. Xu, G Y. Zhou, R C. Sun, J F. Kennedy, “Comparative characterization of degraded and non-degradative hemicelluloses from barley straw and maize stems: Composition, structure, and thermal properties”, *Carbohydrate Polymers.* (2009) 78, 609-619.

- [20] R C. Sun, J. Tomkinson, “Characterization of hemicelluloses obtained by classical and ultrasonically assisted extractions from wheat straw”, *Carbohydrate Polymers*. (2002) 50, 263-271.
- [21] G. Canche´-Escamilla, D. E. Pacheco-Catala´n, S. B. Andrade-Canto, “Modification of properties of rayon fibre by graft copolymerization with acrylic monomers”, *J Mater Sci* (2006) 41, 7296-7301.
- [22] J. Chen, J. Yi, P. Sun, Zhao-T. Liu, “Grafting from ramie fiber with poly(MMA) or poly(MA) via reversible addition-fragmentation chain transfer polymerization”, *Cellulose*. (2009) 16, 1133-1145.
- [23] P. Ghetti, L. Ricca, L. Angelini, “Thermal analysis of biomass and corresponding pyrolysis products”. *Fuel* (1996) 75, 565–73.
- [24] M. Sain, Ayse Alemdar, “Biodegradable nanocomposites from wheat straw”. *In: Proceedings of the AIChE 2006 Annual Meeting. San Francisco, CA, November 12–17, (2006).*
- [25] A X. Jin, J L. Ren, F. Peng, F. Xu, G Y. Zhou, R C. Sun, J F. Kennedy, “Comparative characterization of degraded and non-degradative hemicelluloses from barley straw and maize stems: Composition, structure, and thermal properties”, *Carbohydrate Polymers*. (2009) 78, 609-619.
- [26] P. K. Adapa, C. Karunakaran, L. G. Tabil, G. J. Schoenau, “Qualitative and Quantitative Analysis of Lignocellulosic Biomass using Infrared Spectroscopy”, *CSBE/SCGAB* (2009) CSBE09-307.
- [27] G. Duan, C. Zhang, “Preparation and Characterization of Mesoporous Zirconia Made by Using a Poly (methyl methacrylate) Template”, *Nanoscale Res Lett*. (2008) 3, 118–122.

Chapter 5. Conclusion

Bio composite from natural fibers derived from agricultural waste and/or bio-based polymers is expected as one of the key material to achieve sustainable society. Although, the incompatibility between the hydrophilic natural fiber and hydrophobic polymer matrices diminishes mechanical properties is the barrier for further development. In order to overcome the poor compatibility between the natural fiber and polymer matrices, surface property control techniques such like chemical modification by compatibilizer, vapor-phase assisted surface polymerization (VASP) was investigated. The results obtained through this research were summarized as below:

In chapter 2, Bio composites of polypropylene (PP) and *Erianthus* fiber (ETF) were fabricated using Maleic anhydride-modified polypropylene (MAPP) as a compatibilizer, to improve interfacial adhesion between polymer and fiber. *Erianthus* is cellulose resource crop expected as raw material producing bio-ethanol due to its fast growth and high CO₂ fixation efficiency, but potential as filler unveiled in this study. Since ETF/PP/MAPP composites improved the mechanical properties, it is revealed that interfacial compatibility is critical. Although compatibilizer is common and simple, selection and optimization of compatibilizer upon various combinations of fiber and polymer matrices require much time and money.

In chapter 3, to overcome compatibilizer's problem, vapor-phase assisted surface polymerization (VASP) method was selected as an alternative and more versatile surface modification method. Bio composites of biodegradable poly (L,L-lactide) [PLLA] and wheat straw fiber (WSF) as a representative agricultural waste were fabricated and characterized. VASP of MMA onto WSF was applied to modify surface property (from hydrophilic to hydrophobic) and improve compatibility with PLLA. The interfacial compatibility between

PLLA and WSF using VASP of MMA improved mechanical property and thermal stability of WSF/PLLA composites. VASP could be applicable to various combination of natural fibers (lignocellulosic material) and polymer matrix. However, severe control of operation parameters especially monomer supply under saturated vapor pressure is limiting factor of conventional VASP treatment for further scale up.

In chapter 4, the gas-flow type of vapor-phase assisted surface polymerization (VASP-F) was successfully developed which the substrate surface could be polymerized through monomer mist produced by monomer bubbling. WSF treated by VASP-F also exhibited surface modification same as VASP while treating larger amounts of substrates. VASP-F is advanced and controllable technique to give breakthrough for scale up with monomer recovery. Additionally, tuning of property would be available by block copolymerization owing to the mode of living property during VASP-F.

In conclusion, improvement of compatibility between natural fiber and polymer matrices are essential to produce the high-performance polymer/agricultural waste composites.

This study provides design principle of natural fiber reinforced plastics. Utilization of agricultural waste as a filler for bio composites would lead to sustainable society by achievement of environment conservation, and social change especially encouraging agricultural sector revitalization.

PUBLICATIONS FROM THIS THESIS

Manuscript published

- 1) “セルロース資源作物エリアンサスを利用した高分子複合材の開発”

李 喜星・脇坂 港・長澤 教夫・西田治男・安藤義人

高分子論文集, Vol. 71, No. 1, pp. 31-37 (Jan., 2014)

Manuscript submitted

- 1) “Enhancement of compatibility based on vapor-phase assisted surface polymerization (VASP) method for poly(L,L-lactide) composites with wheat straw fiber”

Heesung Lee ; Minato Wakisaka ; Norio Nagasawa ; Haruo Nishida ; Yoshito Andou

(Will be submitted to Polymer Composites: Decision on Manuscript ID PC-14-0185)

Presentations at National and International Conferences

Poster presentation

- 1) Hee-Sung LEE, Dong-Hee KIM, Song-Soo JANG, Minato WAKISAKA, Yoshito ANDOU, Haruo NISHID; “Design of Bio-based Composite from Waste Agricultural Residue by Vapor-phase Assisted Surface Polymerization(VASP)”. AFORE-1 1st Asia-Pacific Forum on Renewable Energy, 16-19 November 2011, Busan, Korea
- 2) 李 喜星, 金 同希, 安藤義人, 白井義人, 西田治男; “気相重合法によって表面修飾した麦藁繊維を用いたポリ乳酸複合体の機械的及び熱的性質”. 第61回高分子討論会, 19-21 September 2012, Nagoya, JAPAN.
- 3) 李 喜星, 安藤義人, 白井義人, 西田治男, 長澤教夫, 原昌生, 堀井崇良; “未利用農業資源である麦わらの高分子複合材料への利用”. 第21回ポリマー材料フォーラム, 1-2 November 2012, Kyushu, JAPAN.
- 4) 李 喜星, 脇坂 港, 安藤義人, 西田治男; “ガス流動型気相重合法の開発”. 第1回高分子学会グリーンケミストリー研究会シンポジウム, 23-24 August 2012, Tokyo, JAPAN.
- 5) 李 喜星, 脇坂 港, 安藤義人, 西田治男; “ガス流動型気相重合法の開発”. 第27回中国四国支部高分子研究会, 9 November 2012, Yamaguchi, JAPAN.

Oral presentation

- 1) 李 喜星, 脇坂 港, 安藤義人, 西田治男; 気相からのモノマー供給による粉体表面開始重合, 29-31 May 2013, Khoto, JAPAN

Acknowledgement

This work was carried out at Graduate School of Life Science and System Engineering, Kyushu Institute of Technology.

Thanks God, the merciful and the passionate, for providing me the opportunity to step in the science.

I would like to thank Associate Professor Minato Wakisaka, for providing the opportunity to study on this research. I would like to thank for his advice, and contribution

I gratefully thank for Associate Professor Yoshito Andou constructive comments and suggestions, which made him a backbone of this research and so to this thesis.. You're a supervision, advice, crucial contribution, and guidance from the very early stage of this research as well as giving me extraordinary experiences throughout the research. Above all and the most needed, he provided me unflinching encouragement and support in various ways. In addition, your support made this achievement joyful and an excellent experience for me. I express my feelings about the love and patience that I observed from you.

I would like to thank Prof. Haruo Nishida for their advice, supervision. I gratefully thank Prof. Yoshihito Shirai, Associate Professor Tamaki Kato and Dr. Takayuki Tsukegi for his constructive comments and suggestions. Many interesting scientific and non-scientific discussions were always stimulating and will be a good memory of the year I studied in Kyushu Institute of Technology.

I would like to thank Dr. Norio NAGASAWA (NARO Bio-oriented Technology Research Advancement Institution) for the financial and material support to this research.

I am deeply indebted to Dr. Sung-Soo Jang: it has been an invaluable experience to come Japan for me by his suggestion. This thesis would not have been possible without him.

I would like to thank Prof. Sang-Jin Park, for their patience, help, constant support, understanding, love, and helpful discussions.

I would like to thank for my father, mother and sister. I would love to cordially express my gratitude for all of family support. Thanks for everything. Finally, I would like to thank everybody who was important to the successful realization of thesis, as well as expressing my apology that I could not mention personally one by one.

LEE HEESUNG

March 2014